Numerical investigation of pressure and H_2O dilution effects on NO formation and reduction pathways in pure hydrogen MILD combustion

Xu, Shunta; Xi, Liyang; Tian, Songjie; Tu, Yaojie; Chen, Sheng; Zhang, Shihong; Liu, Hao

Published in:
Applied Energy

DOI:
10.1016/j.apenergy.2023.121736

Publication date:
2023

Document Version
Author accepted manuscript

Numerical investigation of pressure and H_2O dilution effects on NO formation and reduction pathways in pure hydrogen MILD combustion

Shunta Xu [a], Liyang Xi [a], Songjie Tian [a], Yaojie Tu [a], Sheng Chen [b], Shihong Zhang [a], Hao Liu [a, *]

[a] *State Key Laboratory of Coal Combustion, School of Energy and Power Engineering, Huazhong University of Science and Technology, Wuhan 430074, China*

[b] *Department of Mechanical Engineering, Glasgow Caledonian University, Glasgow, Scotland G4 OBA, United Kingdom*

*Corresponding author.

E-mail address: liuhao@hust.edu.cn (H. Liu). Tel.: +86 27 58868758; Fax: +86 27 58868759.

Abstract

Pure hydrogen moderate or intense low-oxygen dilution (MILD) combustion offers a potential solution to meet low NO emission needs while achieving rapid decarbonization for gas turbines. This paper reports a numerical investigation of the pressure (1-25 atm) and H_2O dilution (0-60%vol, including its physical and chemical effects) influences on NO formation and reduction pathways in opposed-flow pure hydrogen diffusion MILD combustion, where the present NO sub-pathway analysis method is also evaluated. Results show that, the present NO sub-pathway analysis method with Glarborg2018 can respectively predict thermal NO, prompt NO, NO formed via NNH and N_2O-intermediate, and NO reduced via CH_i and H reburning reasonably well. In pure hydrogen MILD

combustion, NO emission reaches its peak with the pressure up to about 6 atm due to more NO formed via N_2O-intermediate, and then decreases as the pressure is further raised, which is mainly attributed to less NO formation via NNH and more NO reduction by H radicals, finally causing the dominant NO formation pathway to transform from NNH to N_2O-intermediate at high pressure. The addition of H_2O, mainly because of its chemical effect to inhibit the NNH and N_2O-intermediate pathways via the channels NNH+O→NO and N_2O+H/O→NO, results in further NO emission reduction. The top NO contributor is changed from NNH to N_2O-intermediate with H_2O dilution at atmospheric pressure, while at high pressure, NO formation is invariably dominated by the N_2O-intermediate pathway even when H_2O is added up to 60%vol. NO reduction, which is initiated by the channel NO+H(+M)⇌HNO(+M), behaves more actively at high pressure, constituting 21% of the total NO produced at 25 atm, while its importance is weakened with H_2O dilution.

Keywords

MILD combustion, Opposed-flow flame, Hydrogen, Pressure, H_2O dilution, NO reaction pathway.

Graphical abstract

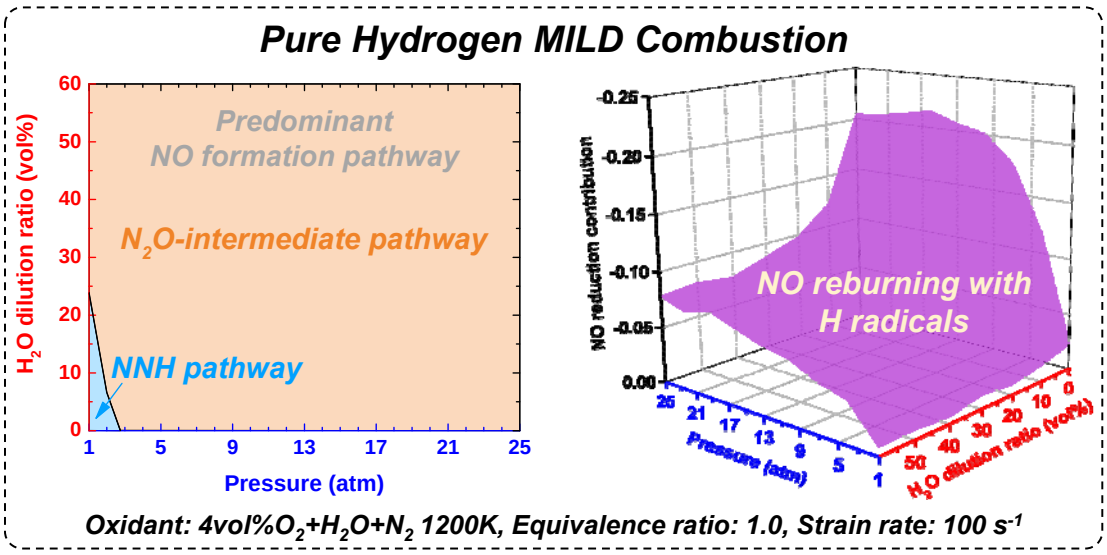

Nomenclature

Acronyms

MILD	Moderate or intense low-oxygen dilution
FLOX	Flameless oxidation
NG	Natural gas
OPPDIF	Opposed-flow diffusion flame
CRN	Chemical reactor network
ROP	Rate of production
JSR	Jet-stirred reactor
EINO	NO emission index

Symbols

FN_2	Factitious nitrogen
FH_2O	Factitious water vapor
P	Pressure
X_{O_2}	Oxygen volume fraction in the oxidant
X_{N_2}	Nitrogen volume fraction in the oxidant
X_{H_2O}	Water vapor volume fraction in the oxidant
X_{FN_2}	Factitious nitrogen volume fraction in the oxidant
X_{FH_2O}	Factitious water vapor volume fraction in the oxidant
U_f	Fuel injection velocity
T_f	Fuel temperature
U_o	Oxidant injection velocity
T_o	Oxidant temperature
T_{si}	Self-ignition temperature of reactants
a_s	Strain rate
L	Separation distance between two impinging nozzles

Greek letters

φ	Equivalence ratio
ρ_f	Fuel density
ρ_o	Oxidant density

1. Introduction

Rapid social-economic development accelerates the consumption of natural gas (NG) in gas turbines, resulting in large emissions of carbon dioxide (CO_2) and further the greenhouse effect [1-3]. To mitigate this effect, hydrogen (H_2), which can be attained from water electrolysis powered by renewable energy sources [4], has been considered as a promising zero-carbon alternative fuel to natural gas for the decarbonized power supply with gas turbines [5]. However, pure hydrogen combustion is prone to generate considerable amounts of nitrogen oxide (NO_x), mainly nitric oxide (NO), because of its high flame temperature [6]. Thermoacoustic instability/oscillation may be also encountered in gas turbines [7-12]. Hence, new clean and efficient hydrogen combustion technologies need to be developed to promote source NO_x reduction while maintaining zero-carbon emissions combined with good combustion stability for gas turbines.

Moderate or intense low-oxygen dilution (MILD) combustion [13], analogous to but not equal to high temperature air combustion [14], flameless oxidation (FLOX) [15], and colorless distributed combustion [16], is a promising low-NO_x combustion technology that can offer a potential solution to achieve NO control/reduction during hydrogen combustion. Considering that reactants are highly diluted by hot combustion products, MILD combustion is distributed throughout a furnace rather than concentrated in a narrow flame front [15], featuring invisible flames, nearly-homogeneous temperature fields, low thermoacoustic oscillations, and good combustion stability [14, 17]. Motivated by these features, the MILD technology has been applied in furnaces [18] and is extending its application to gas turbines [16, 17, 19-23].

Understanding the pressure effects on MILD combustion is mandatory if extending the MILD

technology to gas turbines. Using the FLOX® and COSTAIR burner technology, single-digit NO emissions at atmospheric pressure have been demonstrated by Flamme [19] and Levy et al. [24] reported that low NO emission levels can be also achieved if the pressure is elevated. Lückerath et al. [25] experimentally confirmed the applicability of the FLOX® burner to gas turbine combustors fueled with NG/H_2 mixtures at 20 bar. In the FLOX® combustor, NO emission can be lower than 10 ppm@15%O_2 [26], which can be reduced by elevating the inlet velocity [25]. Huang et al. [27] concluded that the pressure increase reduces OH mole fraction and subsequently causes the fuel oxidation delay in syngas/hydrogen MILD combustion. Khalil and Gupta [28] experimentally observed that as the pressure is increased (1-2.5 atm) at a constant inlet mass flow rate, NO emission is increased inside a methane (CH_4) fueled MILD combustor. Besides higher NO emissions, a departure from the MILD regime may occur with pressure elevation [23, 29-31]. Sadanandan et al. [32] further reported hydrogen addition moves the reaction zone upstream with greater NO emissions in the FLOX® combustor at 20 bar. Shi et al. [33] numerically concluded that NO emission from opposed-flow syngas MILD combustion is reduced as the pressure increases from 1 to 20 atm, mainly resulting from the decrease in NO formation via the NNH pathway.

Table 1. Summary of the investigations on hydrogen-containing natural gas or syngas MILD combustion at elevated pressure or/and H_2O dilution.

Fuel	Oxidant	System	Method[a]	Pressure	NO factor studied	Mechanism	Reference
80/60%NG +20/40%H_2	Air	FLOX® burner	EXP	20 bar	NO emission	/	[25]
60%NG+40 %H_2	Air	FLOX® burner	EXP	20 bar	NO emission	/	[32]
48%CO+38	Air	CRN	SIM	1-19 atm	/	Davis	[27]

%H_2+14%CO_2, H_2						mechanism	
CO/H_2 (1:1)	O_2/N_2, O_2/H_2O/N_2	OPPDIF	SIM	1-20 atm	NO formation	USC-Mech II +GRI-Mech 2.11's NO_x sub-model	[33]
H_2	Air, O_2/N_2/H_2O	OPPDIF	SIM	1 atm	NO emission	GRI-Mech 3.0	[34]

[a] EXP: Experiment, SIM: Simulation.

Increasingly stringent NO emission regulation forces to achieve further NO emission reduction for hydrogen MILD combustion in gas turbines, where water (H_2O) injection is often used to control NO formation [35]. Park et al. [34] numerically observed that the addition of H_2O to the air stream decreases the flame temperature and hence suppresses NO emission in opposed-flow hydrogen/air MILD combustion at atmospheric pressure with GRI-Mech 3.0. de Joannon et al. [36] found that steam dilution significantly influences the reaction zone structures including temperatures and heat releases in opposed-flow methane MILD combustion at 10 bar. Cheong et al. [37] noticed that H_2O addition (0-15%) favors reducing the formation of NO from methane opposed-flow MILD combustion. Shu et al. [38] numerically found that NO is formed mainly via N_2O in methane MILD combustion diluted by H_2O. Si et al. [39] experimentally confirmed that H_2O dilution is more beneficial than N_2 dilution for realizing natural gas MILD combustion, finally leading to lower NO emissions.

Emerging from the above literature review, the previous studies [25, 26, 28, 29, 32, 33] all targeted natural gas and/or hydrogen-containing fuels in high-pressure MILD combustion (see Table 1), whereas they were very less extended to pure hydrogen fuel at high pressure. Importantly, the NO chemistry kinetic is heavily dependent on the hydrogen-blending ratio in MILD combustion [40]. However, during pure hydrogen MILD combustion at high pressure, especially over a wide range

92 covering the operating pressure of typical E-class and state-of-the-art H/J-class heavy-duty gas
93 turbines [41, 42], NO formation and reduction mechanisms were not addressed, especially including
94 NO reburning with H radicals that receives less attention despite hydrogen being capable to be used
95 as a reburn fuel to reduce NO [43], and the quantitative NO sub-pathway analysis method also needs
96 to be evaluated/validated based on experiments. In addition, how the reduction of NO proceeds during
97 pure hydrogen MILD combustion diluted by H_2O was not revealed, let alone the physical and chemical
98 effects of H_2O at different pressures with a recently-developed NO_x sub-model, which is required to
99 be investigated in order to achieve ultra-low and even near-zero NO emissions while maintaining zero
100 CO_2 production for gas turbines.

101 In this work, a computational parametric study using a detailed mechanism recently-proposed by
102 Glarborg et al. [44] in 2018 (termed Glarborg2018) is done to characterize the influence of pressure
103 (1-25 atm) and H_2O dilution (0-60%vol, including its physical and chemical effects) on NO formation
104 and reduction in opposed-flow pure hydrogen diffusion flames during MILD combustion. In particular,
105 the present NO sub-pathway analysis method coupled with Glarborg2018 for predicting NO formation
106 and reduction via six different pathways is evaluated, and then the quantitative NO reaction path
107 diagram analysis for pure hydrogen MILD combustion is performed, and NO formation via thermal,
108 NNH, and N_2O-intermediate pathways as well as NO reduction by H radicals are further investigated
109 at different pressure and H_2O dilution levels.

110 2. Strategy of numerical modeling

111 2.1. Opposed-flow diffusion flames

112 An opposed-flow diffusion flame (OPPDIF) stabilized in a steady, one-dimensional diffusive

layer, where a hot-diluted oxidant flow is employed to impinge on a room-temperature undiluted fuel flow, is used to model MILD combustion with the OPPDIF module in CHEMKIN [45]. The mathematical model used in this geometry has been described in the Supplementary Material. As shown in Figure 1, it consists of two opposed-flow nozzles separated by a finite distance (L), i.e., 1.5 cm. Fuel and oxidant flows are injected through the nozzles with an inside diameter of 20 mm. Due to the impinging impact of these two flows, a stagnation plane is formed, whose location depends on the injection momentums of fuel and oxidant.

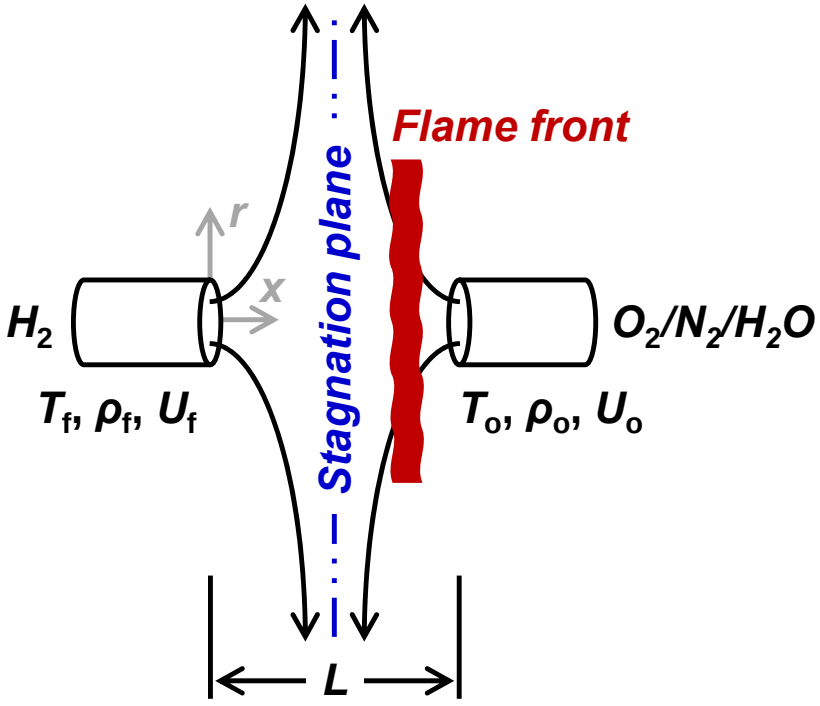

Figure 1. Opposed-flow diffusion reactive configuration to model pure hydrogen MILD combustion.

The strain rate (a_s) is defined as [46]:

$$a_s=\frac{2|u_o|}{L}\left[1+\frac{|u_f|}{|u_o|}\sqrt{\frac{\rho_f}{\rho_o}}\right] \quad (1)$$

where ρ is density, u is gas flow velocity, and the subscripts "f" and "o" refer to fuel and oxidant,

125 respectively.

126 In the study, the opposed-flow flame calculations are performed by solving the gas energy
127 equation. Thermal diffusion and multicomponent transport are considered due to higher calculation
128 accuracy. To ensure converged solutions, adaptive mesh parameters GRAD and CURV are fixed at 0.1
129 and 0.5, respectively. Maximum number of grid points allowed is set as 350 to save computational cost
130 while ensuring solution accuracy. Absolute and relative tolerances are specified as 10^{-9} and 10^{-5},
131 respectively.

132 2.2. Model validation

133 Lots of reaction models have been developed for hydrogen and small hydrocarbon fuels, such as
134 GRI-Mech 2.11 [47], GRI-Mech 3.0 [48], Li mechanism [49], Davis mechanism [50], USC-Mech II
135 [51], Konnov 0.6 [52], and Glarborg2018 [44] often used. Among them, GRI-Mech is a classical and
136 widely-used reaction model for simulating the combustion of hydrocarbon and even hydrogen fuels
137 [34, 37, 38]. The models of Li et al. [49], Davis et al. [50], and USC-Mech II [51] were proposed for
138 hydrogen or hydrogen-containing fuels, while they lack NO_x chemistry. Konnov 0.6 [52] is applicable
139 to hydrogen/hydrocarbon fuels, including 129 species and 1231 reactions with nitrogen chemistry.
140 Glarborg2018 is a detailed reaction model recently-developed by Glarborg et al. [44], which consists
141 of 151 species and 1397 reactions with a detailed NO_x sub-model where the NNH/N_2O reaction subsets
142 that are important, especially in hydrogen flames, have been updated.

143 In this study, the commonly-used kinetic mechanisms with nitrogen chemistry, i.e., GRI-Mech
144 2.11, GRI-Mech 3.0, Konnov 0.6, and Glarborg2018, are chosen for model validation. The ability of
145 these mechanisms to predict NO from pure hydrogen combustion is first validated against the

experimental data of Rørtveit et al. [53]. Figure 2 shows the predicted and measured temperature and NO mole fraction profiles in opposed-flow H_2/air diffusion flames at atmospheric pressure [53]. It is obvious in Figure 2 that the temperature profiles can be captured by all the reaction models with reasonable accuracy, whereas they perform very differently in NO prediction. In particular, the peak NO level is highly overestimated by GRI-Mech 2.11/3.0 as well as Konnov 0.6, while the NO predicted by Glarborg2018 is in better agreement with that observed experimentally in terms of its peak level and profile.

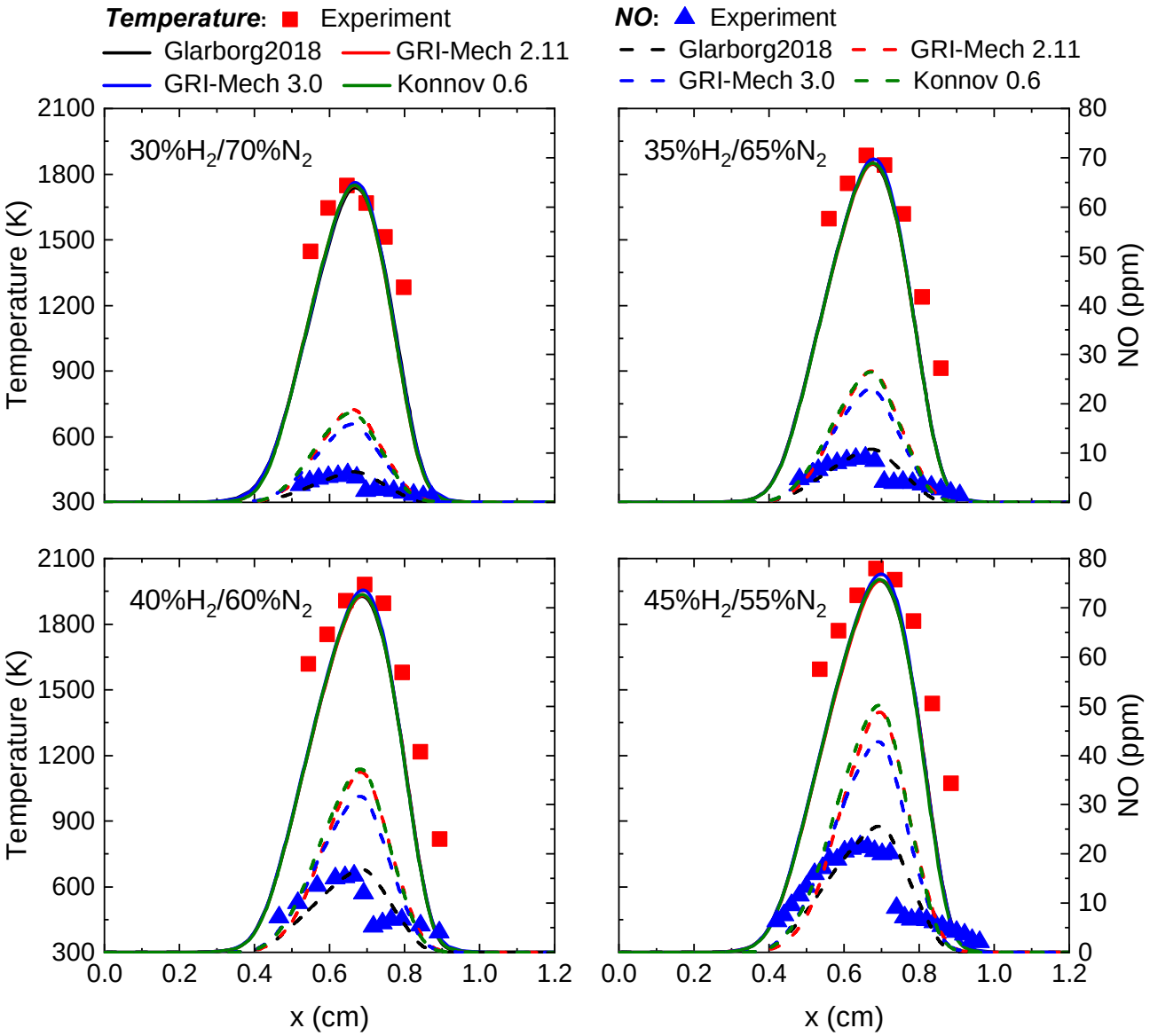

Figure 2. Measured [53] and predicted temperature and NO mole fraction in opposed-flow

H_2/air diffusion flames at atmospheric pressure.

To our best knowledge, there are no available experimental data of NO for opposed-flow H_2/air flames at high pressure. Accordingly, the experiment of high-pressure opposed-flow CH_4/H_2/air flames from de Persis et al. [54] is used to further check the Glarborg2018 predictability for NO at high pressure. Figure 3 plots the measured and predicted NO mole fraction profiles in opposed-flow CH_4/H_2/air flames at high pressure, which reveals that Glarborg2018 behaves reasonably well in the prediction of NO including its peak level and profile at elevated pressures up to 7 atm. Although the mechanism validation at high pressure is carried out based on a hydrogen-blending fuel rather than a pure hydrogen fuel, it can still demonstrate that Glarborg2018 has the predictive ability for hydrogen oxidation at high pressure, since the H_2/O_2 reaction subset is the fundamental kinetic in any hydrocarbon model.

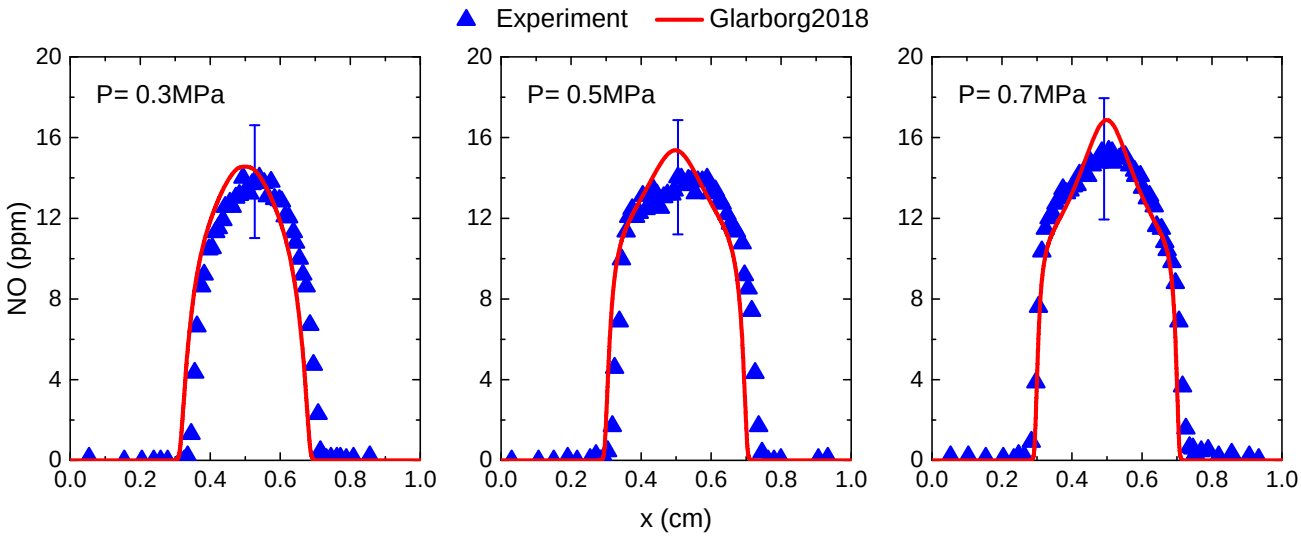

Figure 3. Measured [54] and predicted NO mole fractions in opposed-flow CH_4/H_2/air flames with 20%vol hydrogen at high pressures.

As a whole, Glarborg2018 shows the best predictability for NO formation in hydrogen combustion at atmospheric and high pressures and therefore it is used in this study.

2.3. Operation parameters

Table 2 gives the operating conditions, where X_{O_2}, X_{N_2}, X_{H_2O}, X_{FN_2}, and X_{FH_2O} are the volume fraction of O_2, N_2, H_2O, FN_2, and FH_2O in the oxidant, respectively. For all the cases studied, the fuel/air equivalence ratio (φ) at the nozzle inlet is maintained at 1.0 due to its significant effect on NO formation and reduction [40]. Hydrogen is fed as a fuel with a fixed injection velocity U_f = 1.48 cm/s at room temperature (i.e., fuel temperature (T_f) of 300 K), corresponding to Reynolds numbers of about 27-670 at 1-25 atm, and oxygen diluted by N_2 and H_2O as the oxidant is introduced at a preheated oxidant temperature (T_o) of 1200 K with an injection velocity U_o equal to 74.21 cm/s corresponding to a strain rate (a_s) of 100 s^{-1} (following the study of Rørtveit et al. [53]). Note that all the cases in Table 2 satisfy the definition of MILD combustion proposed by Cavaliere and de Joannon [13], where T_o is higher than the self-ignition temperature of reactants (T_{si}) but the temperature increase is lower than T_{si}, which indicates the occurrence of MILD combustion.

Table 2. Cases investigated.

	Fuel	Oxidant (vol%)					P (atm)	φ	U_f (cm/s)	U_o (cm/s)	a_s (s^{-1})
		X_{O_2}	X_{N_2}	X_{H_2O}	X_{FN_2}	X_{FH_2O}					
Series 1	H_2	4	96				1-25	1.0	1.48	74.21	100
Series 2	H_2	4	36-96	0-60			1	1.0	1.48	74.21	100
Series 3	H_2	4	36-96		0-60		1	1.0	1.48	74.21	100
Series 4	H_2	4	36-96			0-60	1	1.0	1.48	74.21	100
Series 5	H_2	4	36-96	0-60			12	1.0	1.48	74.21	100
Series 6	H_2	4	36-96		0-60		12	1.0	1.48	74.21	100
Series 7	H_2	4	36-96			0-60	12	1.0	1.48	74.21	100

In this work, the pressure (P) is increased from 1 to 25 atm (covering the operating pressure of typical E-class and state-of-the-art H/J-class gas turbines [41, 42]) to figure out the pressurized effects on NO formation and reduction in pure hydrogen MILD combustion, corresponding to Series 1 in Table 2. The H_2O mole fraction in the oxidant (X_{H_2O}) is varied from 0 to 60% at 1 and 12 atm (based on the operating pressure of typical E-class gas turbines [41]) to examine the effect of H_2O dilution, corresponding to Series 2 and 5 in Table 2. To further identify the physical and chemical effects of H_2O, two artificial and chemically inert species, i.e., a fake nitrogen species (FN_2) and a fake water species (FH_2O), are introduced. These two species have the same thermodynamical and transport properties as N_2 and H_2O, respectively, but do not participate in reactions. Note that, the fake species FN_2 is considered to eliminate the effect of the N_2 concentration decrease when H_2O is added to replace N_2 in the oxidant. The differences between FH_2O and FN_2 are attributed to the physical effect of H_2O due to the deviation of its physical properties from those of N_2. The differences between H_2O and FH_2O addition are attributed to the chemical effect of H_2O. In Table 2, Series 3-4 and 6-7 are set to grasp the physical and chemical effects of H_2O on NO formation and reduction pathways in pure hydrogen MILD combustion.

3. NO sub-pathway analysis method and its performance evaluation for predicting the NO formed and reduced via different pathways

3.1. NO sub-pathway analysis method

To examine the effect of each pathway on NO production separately, the NO sub-pathway analysis method developed by Xu et al. [40, 55], which was first proposed for hydrogen-free fuels [55] and then further extended to hydrogen-containing and/or pure hydrogen fuels [40], is adopted in this study.

As suggested in our recent works [40, 55], the key reaction subsets of thermal, prompt, NNH, and N_2O-intermediate mechanisms as well as NO reduction by hydrocarbon and non-hydrocarbon fragments for Glarborg2018 are categorized in Table 3, where the pathways of NO reburning with hydrocarbon fragments (e.g., C, CH, CH_2, CH_3, and HCCO) and non-hydrocarbon fragments (e.g., H) are referred to as CH_i reburning and H reburning, respectively.

Table 3. Main reaction subsets for thermal, prompt, NNH, N_2O-intermediate, H reburning, and CH_i reburning pathways in Glarborg2018.

Route	Reaction	No.	Reaction	No.	Reaction	No.
Thermal	$N+NO \rightleftharpoons N_2+O$	R674	$N+O_2 \rightleftharpoons NO+O$	R673	$N+OH \rightleftharpoons NO+H$	R672
Prompt	$CH+N_2 \rightleftharpoons NCN+H$	R944	$CH+N_2 \rightleftharpoons HNCN$	R945	$NCN+M \rightleftharpoons C+N_2+M$	R1002
	$CH_3+N \rightleftharpoons H_2CN+H$	R925				
NNH	$NNH \rightleftharpoons N_2+H$	R675	$NNH+O \rightleftharpoons N_2O+H$	R677	$NNH+O_2 \rightleftharpoons N_2+HO_2$	R681
	$NNH+O \rightleftharpoons N_2+OH$	R678	$NNH+O \rightleftharpoons NH+NO$	R679		
N_2O-intermediate	$N_2O+O \rightleftharpoons N_2+O_2$	R763	$N_2O+O \rightleftharpoons NO+NO$	R762	$N_2O+H \rightleftharpoons N_2+OH$	R761
	$N_2O+OH \rightleftharpoons N_2+HO_2$	R764	$N_2O(+M) \rightleftharpoons N_2+O(+M)$	R760	$NH+NO \rightleftharpoons N_2O+H$	R667
H reburning	$NO+H(+M) \rightleftharpoons HNO(+M)$	R720				
CH_i reburning	$CH_3+NO \rightleftharpoons HCN+H_2O$	R930	$CH_3+NO \rightleftharpoons H_2CN+OH$	R931	$CH_2+NO \rightleftharpoons HCNO+H$	R937
	$CH_2+NO \rightleftharpoons HCN+OH$	R938	$HCCO+NO \rightleftharpoons HCNO+CO$	R997	$HCCO+NO \rightleftharpoons HCN+CO_2$	R998
	$CH_2(S)+NO \rightleftharpoons HCN+OH$	R941	$CH_2(S)+NO \rightleftharpoons CH_2+NO$	R942	$CH+NO \rightleftharpoons CO+NH$	R948
	$CH+NO \rightleftharpoons NCO+H$	R949	$CH+NO \rightleftharpoons HCN+O$	R950	$CH+NO \rightleftharpoons CN+OH$	R951
	$CH+NO \rightleftharpoons HCO+N$	R952	$C+NO \rightleftharpoons CN+O$	R956	$C+NO \rightleftharpoons CO+N$	R957
	$C_2H_3+NO \rightleftharpoons HCN+CH_2O$	R979	$C_2H+NO \rightleftharpoons HCN+CO$	R985	$C_2H+NO \rightleftharpoons CN+HCO$	R986
	$C_2+NO \rightleftharpoons C_2O+N$	R989	$C_2O+NO \rightleftharpoons CO+NCO$	R1000	$HCNO+H \rightleftharpoons HCN+OH$	R866
	$HCNO+O \rightleftharpoons HCO+NO$	R867	$HCNO+O \rightleftharpoons NCO+OH$	R868	$HCNO+OH \rightleftharpoons CO+H_2NO$	R869
	$HCNO+OH \rightleftharpoons HCO+HNO$	R870				

Five simulations need to be done for each hydrogen flame to estimate the relative importance of each pathway, as presented in Table 4. In the first simulation (SIM1), the full mechanism is used, while the second (SIM2), third (SIM3), and fourth (SIM4) simulations are done using the full mechanism

without the initiation reactions of the H reburning pathway, without the initiation reactions of the H reburning and NNH pathways, without the initiation reactions of the H reburning, NNH, and N_2O-intermediate routes, respectively. The NO contributed by the H reburning, NNH, and N_2O-intermediate pathways is acquired by differentiating SIM1 with SIM2, SIM2 with SIM3, and SIM3 with SIM4, respectively. Thermal NO is predicted by the fifth simulation (SIM5) using the full mechanism with the NO_x sub-model only involving the three key reactions of thermal NO. Due to the absence of hydrocarbon species, the sub-mechanisms of prompt NO and CH_i reburning are disabled and thus omitted in the NO pathway analysis for pure hydrogen-firing cases.

Table 4. Model processing procedure for pure hydrogen fuel.

	Model processing procedure
SIM1	Full mechanism
SIM2	Deleting the initiation reaction of the H reburning pathway
SIM3	Deleting the initiation reactions of the H reburning and NNH pathways
SIM4	Deleting the initiation reactions of the H reburning, NNH, and N_2O-intermediate pathways
SIM5	Only remaining the initiation reactions of the thermal-NO pathway

3.2. Performance evaluation of the NO sub-pathway analysis method

To ensure the validity of the NO pathway analysis, the present NO sub-pathway analysis method with Glarborg2018 needs to be systematically evaluated for predicting the NO formed/reduced via the thermal, prompt, N_2O-intermediate, NNH, as well as CH_i and H reburning pathways, respectively. To this end, we choose the experimental data of NO from CH_4 or H_2 combustion [56-61] obtained under special conditions that favor NO formation via one of the above six pathways each time. Figure 4(a)-

(f) plots the predicted NO concentrations using the full Glarborg2018 mechanism with or without the initiation reactions (see Table 3) for one of the above six pathways against the experimental data [56-61].

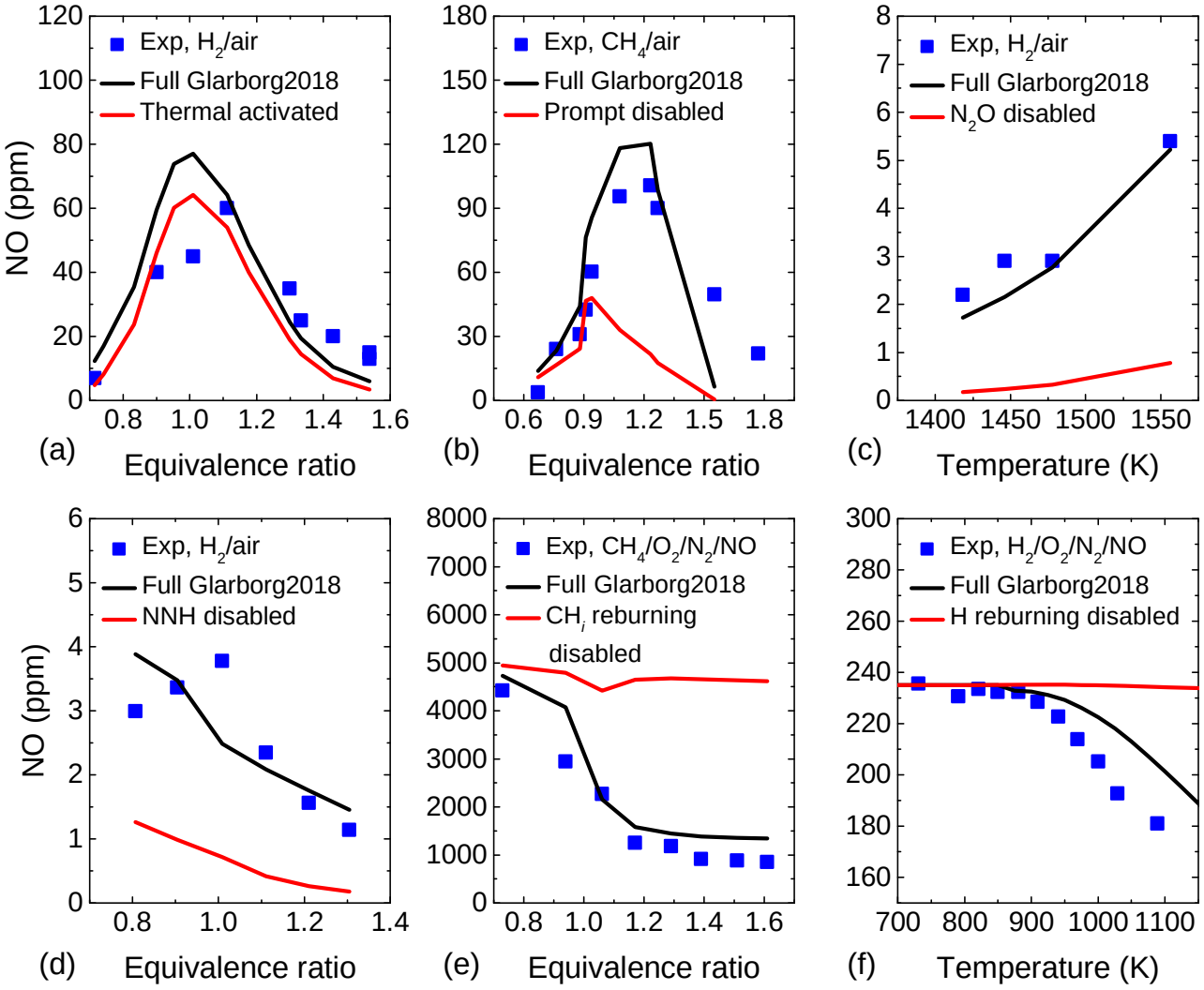

Figure 4. Performance evaluation of the NO sub-pathway analysis method with Glarborg2018 for predicting the NO formed/reduced via different pathways against the experimental data [56-61]: (a) Thermal-NO, (b) Prompt-NO, (c) N_2O-intermediate, (d) NNH, (e) CH_i reburning, (f) H reburning.

3.2.1. Thermal-NO

Thermal-NO mechanism often dominates NO formation in high-temperature combustion typically above 1800 K [62]. Figure 4(a) shows the measured [56] and predicted NO from H_2/air combustion in a jet-stirred reactor (JSR) at 1830-2210 K, where if only the thermal-NO initiation reactions are activated, NO is still predicted without a large decrement. NO is also contributed from N_2O-intermediate/NNH under fuel-lean/fuel-rich conditions, which is responsible for the difference between both models.

3.2.2. Prompt-NO

The JSR measurements of NO from CH_4/air combustion at φ=0.6-1.8 [57] are compared in Figure 4(b) to check the prompt-NO prediction. It is found that if the prompt-NO initiation reactions are removed from Glarborg2018, NO is still predicted well under fuel-lean conditions but highly underestimated under stoichiometric/rich conditions, since prompt NO is the major NO source in stoichiometric/rich conditions [44].

3.2.3. N_2O-intermediate

The JSR experimental data of NO from lean H_2/air combustion (φ=0.6-0.7) at 1400-1550 K [58], where NO is formed mainly via the N_2O-intermediate mechanism, is used. Figure 4(c) shows that if the N_2O-intermediate initiation reactions are deleted from Glarborg2018, NO is severely underpredicted and close to zero at low temperatures. Thermal NO is responsible for the phenomenon where a small amount of NO is still predicted at higher temperatures without the N_2O-intermediate mechanism.

3.2.4. NNH

Due to the predominant role of the NNH mechanism in forming NO at low-temperature and rich conditions [63], the experimental NO data of H_2/air combustion at 1635 K and φ=0.8-1.3 from Purohit et al. [59] are compared in Figure 4(d). When the NNH initiation reactions are disabled from Glarborg2018, NO is found still emitted under fuel-lean conditions but notably underpredicted under reducing conditions, especially for rich mixtures.

3.2.5. CH_i reburning

To evaluate the prediction performance of NO reduction by hydrocarbon fragments, Figure 4(e) shows the comparison of the measured NO from combustion of CH_4 doped with 5000 ppm NO at 1580 K in a JSR [60] with the predictions. It is found that NO does not be reduced and is close to 5000 ppm over the whole φ range when the CH_i reburning reaction subsets is disabled in Glarborg2018.

3.2.6. H reburning

The JSR experimental data of NO as a function of temperature from 700 to 1150 K during the oxidation of a 1% $H_2/O_2/N_2$/NO mixture doped with 235 ppm NO at φ=1.5 [61] are compared in Figure 4(f) to evaluate NO reduction by H radicals. If the H reburning initiation reaction is omitted from Glarborg2018, NO reduction does not occur and NO almost remains at a constant value close to 235 ppm doped initially.

Based on the above analysis, it is concluded that the present NO sub-pathway analysis method with Glarborg2018 can respectively predict NO formation via thermal, prompt, N_2O-intermediate, and NNH pathways as well as NO reduction via CH_i and H reburning pathways reasonably well.

4. Results and discussion

4.1. Quantitative NO reaction path diagram analysis

The quantitative NO reaction pathway diagram analysis is first performed with Glarborg2018 to get an overall recognition of the NO chemistry kinetic for pure hydrogen MILD combustion. Figure 5 shows the pathways forming and reducing NO in pure hydrogen MILD combustion at X_{O_2}= 4%, a_s= 100 s^{-1}, and P= 1 atm, where the reaction rate of each pathway is obtained by integrating the net production or consumption rate over the separation distance between the fuel and oxidant nozzles and the channels with overall rates less than 1.0×10^{-11} mol·cm^{-3}·s^{-1} are omitted.

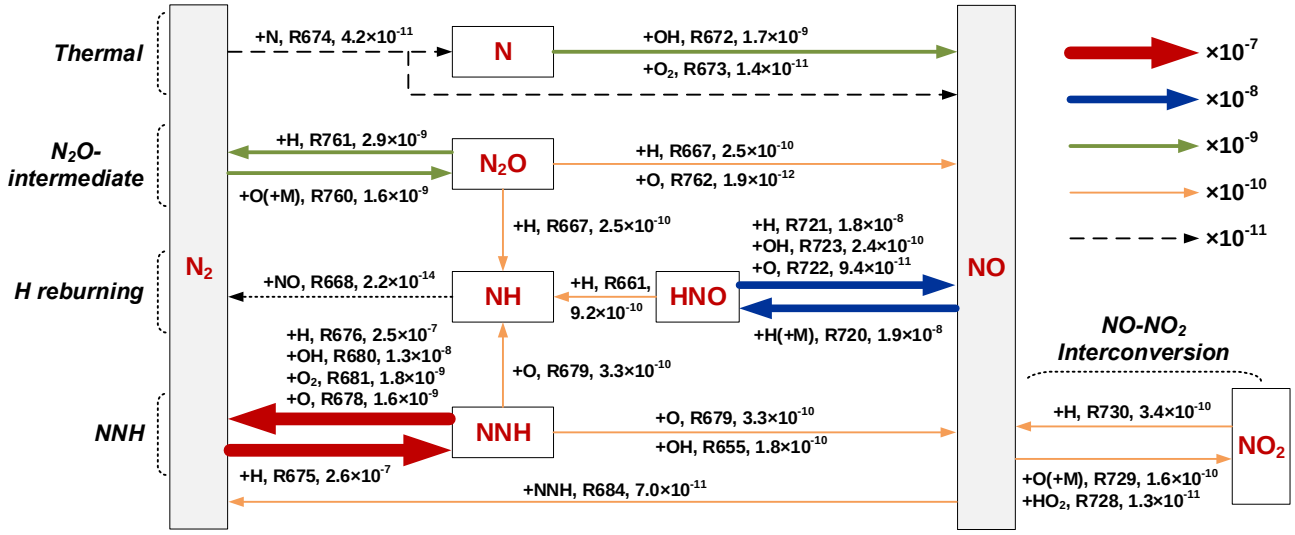

Figure 5. Quantitative reaction path diagram showing NO chemistry in pure hydrogen MILD combustion at X_{O_2} = 4%, a_s = 100 s^{-1}, and P = 1 atm (Unit: mol·cm^{-3}·s^{-1}).

As seen in Figure 5, during pure hydrogen MILD combustion, NO is formed mainly through the thermal, N_2O-intermediate, and NNH pathways, based on the initiation reactions by which N_2 is converted to N or other N-containing intermediate species. The thermal-NO mechanism [62], which proceeds via the pathway $N_2 \xrightarrow{+O} N \xrightarrow{+O_2,\,OH} NO$, controlled by a set of temperature-dependent channels:

N_2+O→NO (R674), N+O_2→NO (R673), and N+OH→NO (R672). Figure 5 reveals that the rate of production (ROP) of the initiation reaction N+NO⇌N_2+O (R674) is lower due to the low reaction temperature. The N_2O-intermediate mechanism [64], mainly via the pathway $N_2 \xrightarrow{+O(+M)} N_2O \xrightarrow{+O,\ H} NO$, is initiated by the reaction N_2+O→N_2O (R760) and then the N_2O formed is partially converted to NO by combining H/O radicals via the channels N_2O+H→NO (R667) and N_2O+O→NO (R762). NO is also yielded via NNH, which is initiated by the reactions of N_2 with H radicals via N_2+H→NNH (R675), and the NNH produced is further oxidized to NO with O radicals via NNH+O→NO (R679). In addition to the channel NNH+O→NO (R679), NNH is also consumed by OH to form NO via the backward reaction of NH_2+NO⇌NNH+OH (R655). This is the NNH mechanism [65] mainly via the pathway $N_2 \xrightarrow{+H} NNH \xrightarrow{+O,\ OH} NO$.

The NO formed is also reduced by atomic hydrogen, which is initiated by the reaction NO+H(+M)⇌HNO(+M) (R720) to yield the intermediate species HNO, and HNO is subsequently converted to NH via HNO+H→NH (R661), followed by reducing NO with NH via NH+NO→N_2 (R668). This is the mechanism of NO reburning with H radicals (i.e., H reburning), mainly via the pathway $NO \xrightarrow{+H} HNO \xrightarrow{+H} NH \xrightarrow{+NO} N_2$. Besides the above four mechanisms, the interconversion between NO and NO_2 also occurs through the following reactions NO+HO_2⇌NO_2+OH (R728), NO+O(+M)⇌NO_2(+M) (R729), and NO_2+H⇌NO+OH (R730). Figure 5 reveals that almost all the reactions giving the production or consumption of NO involve reactions with one of O, H, and OH radicals, i.e., main agents of NO production/consumption, where O, H, and OH radicals are produced from the H_2/O_2 chain reactions H+O_2⇌O+OH (R1), O+H_2⇌OH+H (R3), OH+H_2⇌H+H_2O (R4), and OH+OH⇌O+H_2O (R5).

In general, for pure hydrogen MILD combustion, NO is formed mainly via the NNH ($N_2 \xrightarrow{+H} NNH \xrightarrow{+O,\ OH} NO$) and N_2O-intermediate ($N_2 \xrightarrow{+O(+M)} N_2O \xrightarrow{+O,\ H} NO$) pathways and reduced via the H reburning pathway ($NO \xrightarrow{+H} HNO \xrightarrow{+H} NH \xrightarrow{+NO} N_2$), and the thermal-NO pathway is less active due to low combustion temperatures. The prompt-NO mechanism [66] is disabled and the classical NO reburning mechanism [67] with hydrocarbon fragments is ineffective, due to the absence of hydrocarbon species.

4.2. Pressure effects

In this section, the effect of pressure from 1 to 25 atm (covering the operating pressure range of typical E-class and state-of-the-art H/J-class heavy-duty gas turbines [41, 42]) on NO formation and reduction pathways during pure hydrogen MILD combustion is characterized at X_{O_2}= 4%, T_o= 1200 K, and a_s= 100 s^{-1}, namely Series 1 in Table 2.

4.2.1. Opposed-flow diffusion reactive structures

Figure 6 shows the profiles of temperature and NO in opposed-flow pure hydrogen flames under MILD conditions. At higher pressure, the reacting flow structure moves towards the fuel side and becomes thinner (see Figure 6(a)), thus causing a decrease in the width of the NO profile (see Figure 6(b)). Since the thickness of diffusion flames is of the order of $(D/a_s)^{1/2}$ [68] and the mixture diffusion coefficient (D) is inversely proportional to pressure, the flame thickness is reduced at high pressure. Besides, the peak temperature increases appreciably from 1655 to 1743 K with the pressure from 1 to 10 atm, due to higher reaction intensity. Above 10 atm, the temperature increase is not as significant and the peak temperature tends to level off with the pressure.

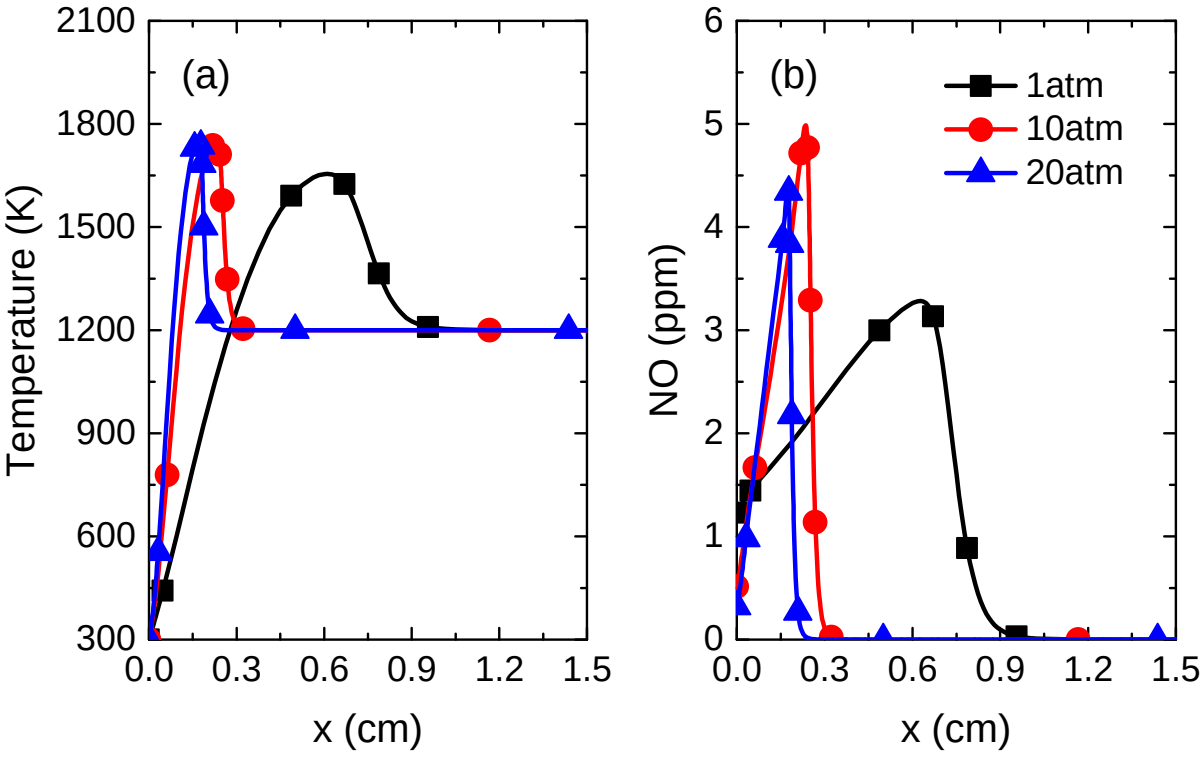

Figure 6. Temperature and NO profiles in pure hydrogen MILD combustion at 1, 10, and 20 atm.

As presented in Figure 6(b), pure hydrogen MILD combustion yields a single-digit NO peak at all pressures. As the pressure rises from 1 to 25 atm, the peak NO mole fraction is increased first and then reduced, following the opposite trend as the peak temperature at high pressure, which implies that NO production is dominated by other mechanisms rather than the thermal-NO mechanism.

4.2.2. NO formation and reduction pathways

To grasp the pressure effects on NO chemistry, NO formation and destruction via different routes are separately characterized in Figure 7, where the profiles of the NO formed via thermal, NNH, and N_2O-intermediate pathways as well as the NO reduced via H reburning pathway are plotted versus the mixture fraction. Regardless of the pressure, the NO mole fraction increases first and then decreases with the mixture fraction from 0 to 1, and the NO formed via all pathways reaches its peak close to the

flame front. Although the peak NO mole fraction exhibits a non-monotonous variation with the pressure, increasing the pressure leads to a monotonous reduction in the net NO mole fraction (gray color) on the fuel-rich side of the flame sheet. This occurs perhaps because of the reduction in the NO formed via NNH, and/or the enhancement of NO reduction by H atoms. At 1 atm, NO is formed mainly via the NNH and N_2O-intermediate routes, which matches the observation in a well-stirred reactor [40], and the thermal-NO route is less important due to the low reaction temperature. As the pressure increases, the amount of the NO contributed by the N_2O-intermediate route rises first and then drops while that contributed by the NNH route reduces monotonously. The thermal-NO route is enhanced at high pressure but such an increase is limited owing to its strong temperature dependence. In addition, NO reduction by H radicals is much more noticeable on the fuel-rich side, due to its higher effectiveness of NO reduction under reducing conditions [40, 69, 70], and it tends to become more appreciable at high pressure.

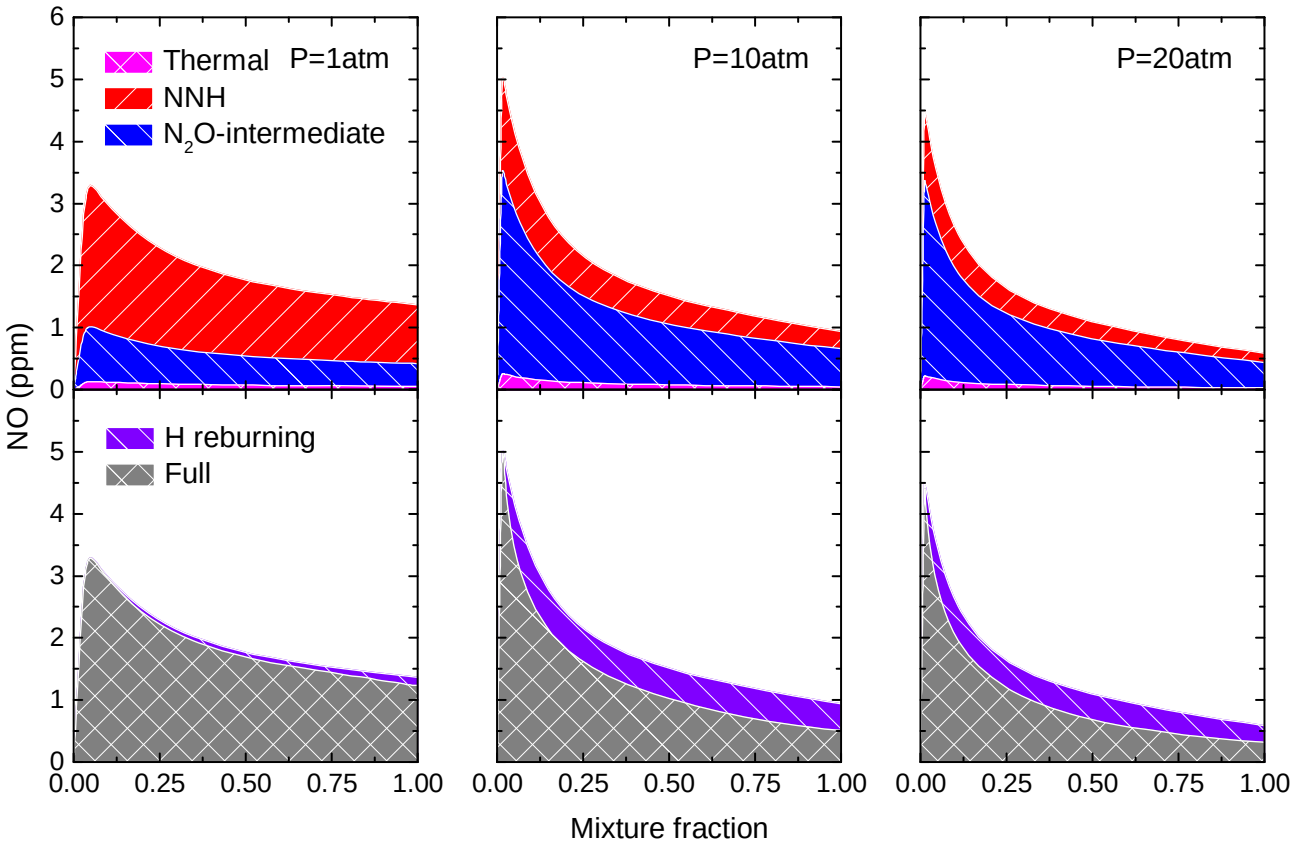

Figure 7. Profiles of the NO formed and reduced via different pathways against mixture fraction in pure hydrogen MILD combustion at 1, 10, and 20 atm.

The global NO emission index (EINO) is used to further characterize the absolute and relative amount of the NO formed or destructed over a wide range of pressures, which is defined as [71]:

$$\mathrm{EINO\ (g\text{-}NO/kg\text{-}Fuel)} = \frac{\int_0^L \dot{\omega}_{\mathrm{NO}} M_{\mathrm{NO}} dx}{-\int_0^L \dot{\omega}_{\mathrm{Fuel}} M_{\mathrm{Fuel}} dx} = \frac{\int_0^L \dot{\omega}_{\mathrm{NO}} M_{\mathrm{NO}} dx}{-\int_0^L \dot{\omega}_{\mathrm{H_2}} M_{\mathrm{H_2}} dx} \quad (2)$$

Here, M_i is the molecular weight, $\dot{\omega}$ the rate of production or consumption, L the separation distance between the two nozzles, and x the axial coordinate.

Figure 8 shows the variation of absolute and relative amounts of the EINO contributed by the thermal, NNH, N_2O-intermediate, and H reburning routes with the pressure from 1 to 25 atm. As plotted in Figure 8(a), the sum of the EINO produced via all the sub-pathways (termed Sum) almost agrees with that of the full mechanism (termed Full), which demonstrates that the present NO sub-

370 pathway analysis method is reliable with a good decoupling effect among NO sub-mechanisms. Figure
371 8(a) reveals that the total EINO presents an increasing trend with the pressure up to about 6 atm due
372 to more NO formed via N_2O-intermediate, followed by a decreasing trend with further increasing
373 pressure to 25 atm, which is mainly attributed to lower NO formation via NNH and higher NO
374 reduction by H radicals. Somewhat differently, Shi et al. [33] reported the total EINO presents a
375 monotonic decreasing trend with pressure from 1 to 20 atm in syngas MILD combustion using the
376 NO_x sub-model from GRI-Mech 2.11, due to the decrease in the NO formed via NNH higher than the
377 increase via N_2O. Such a difference may be caused by the use of different NO_x sub-models. Indeed,
378 the low formation rate of the NNH pathway determined by Glarborg2018 refers to the study of
379 Klippenstein et al. [72], who reported that the importance of the NNH mechanism in forming NO may
380 be overestimated in the kinetic reaction mechanism developed earlier. Overall, the underlying reason
381 for a rise and then a drop in EINO with pressure may be the synergistic interaction between the total
382 NO production rate and the reaction zone size. At high pressure, the NO production rate is promoted,
383 while the reaction zone is concentrated (Figure 6(a)). When the pressure rises slightly, the reduction of
384 the reaction zone is not very significant, which generally leads to a rise in EINO when the pressure
385 starts to increase. However, the considerable reduction of the reaction zone when the pressure increases
386 significantly, to some extent, offsets the impact of the increase in the NO production rate, which causes
387 the drop in EINO at higher pressure.

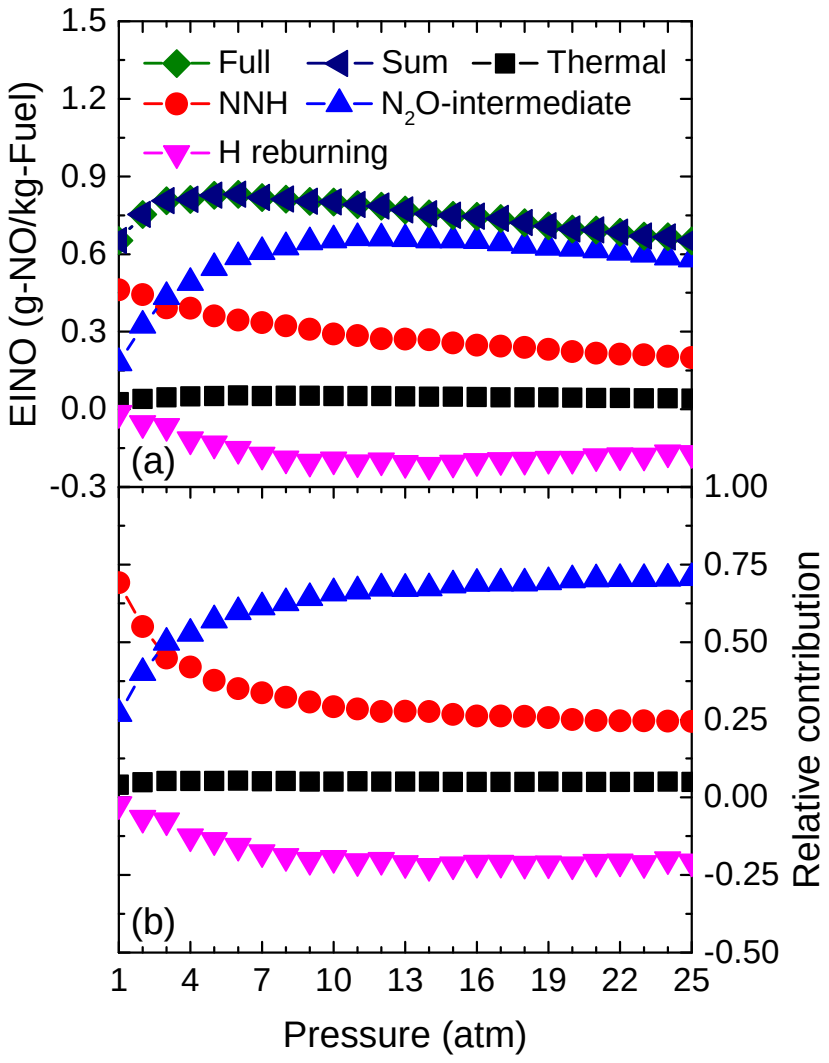

Figure 8. NO formation and reduction characteristics in pure hydrogen MILD combustion at pressure from 1 to 25 atm.

Another observation in Figure 8(a) is that the EINO value is comparable between 1 and 25 atm, which implies that higher pressure is favorable to the reduction of NO emission for pure hydrogen MILD combustion. It is recommended to operate at a higher pressure for minimizing NO emission under the premise of ensuring the realization of pure hydrogen MILD combustion.

Figure 8(b) further exhibits the relative contribution of these pathways to the total NO production at pressures of 1-25 atm. Sensitivity analysis is done to ascertain the important reactions responsible for NO formation and reduction, as displayed in Figure 9. It can be noticed that the NNH route mainly

via the channels NNH+O/OH→NO, where the NNH radicals are solely produced by the channel N_2+H (R675), controls the total NO production at atmospheric pressure, which contributes to 69% of the total NO produced. This study is further extended to high pressure based on our recent research [40]. Figure 9 reveals that as the pressure increases from 1 to 25 atm, the role of NNH+O⇌NH+NO (R679) and NH_2+NO⇌NNH+OH (R655) in forming NO is weakened, causing the relative importance of the NNH route to reduce from 69 to 24%. However, the importance of the N_2O-intermediate route via N_2O(+M)⇌N_2+O(+M) (R760), NH+NO⇌N_2O+H (R667), and N_2O+O⇌NO+NO (R762) increases. With the pressure up to nearly 3 atm, the relative contribution of the NNH and N_2O-intermediate routes on NO formation is comparable, and further increasing pressure leads to the transition of the predominant NO formation pathway from NNH to N_2O; at 25 atm, the contribution makes up 71% for the N_2O-intermediate route. On the other hand, the NO reburning with H radicals, which acts mainly via the pathway $NO \xrightarrow{+H} HNO \xrightarrow{+H} NH \xrightarrow{+NO} N_2$, has the potential to reduce 2-21% of the total NO produced over a wide range of pressures from 1 to 25 atm, and it becomes increasingly important at high pressure (see Figure 8), due to the higher sensitivity of the initiation step NO+H(+M)⇌HNO(+M) (R720) for NO reduction.

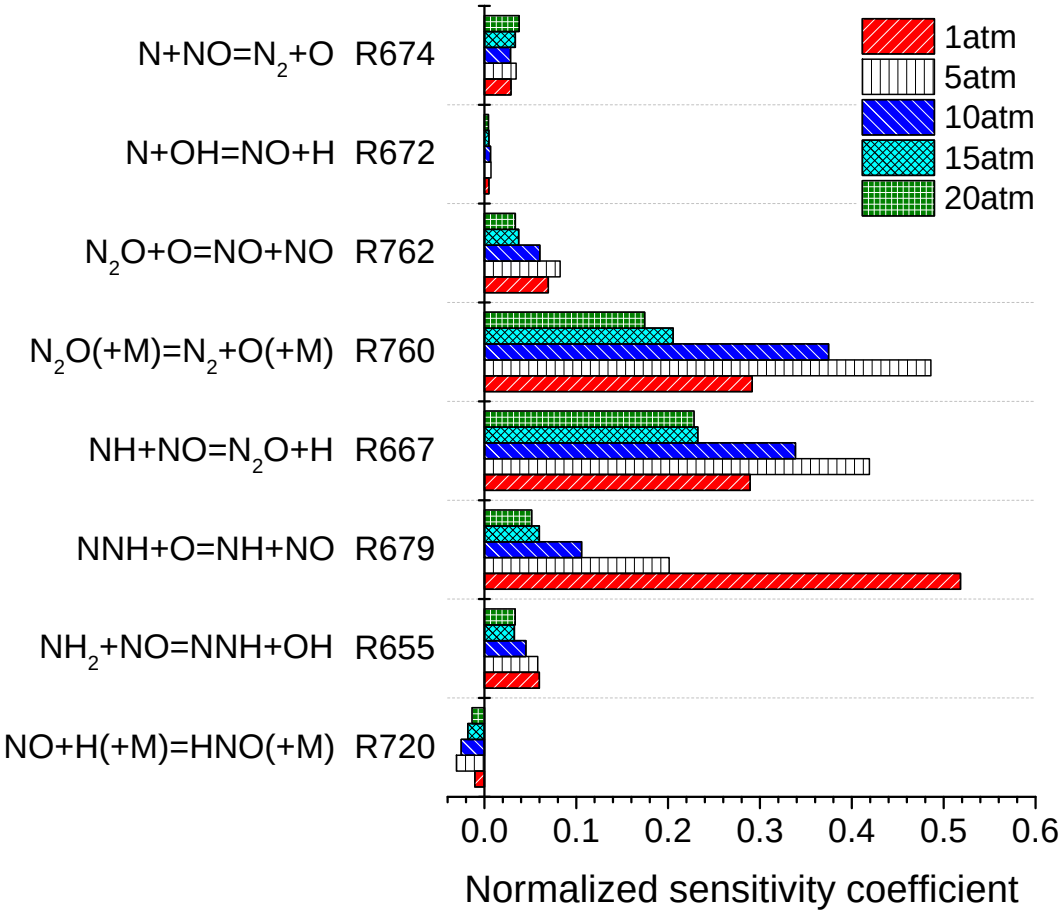

Figure 9. Sensitivity coefficient of the key NO reactions in pure hydrogen MILD combustion at different pressures.

4.3. Physical and chemical effects of H_2O dilution

There is an ongoing need for NO reduction for pure hydrogen MILD combustion to achieve the goal of ultra-low and even near-zero NO emissions. Although H_2O dilution is known to be favorable for reducing NO emission [34, 53], it is still crucial to reveal how the reduction of NO proceeds during pure hydrogen MILD combustion if diluted by H_2O.

4.3.1. Characteristics of the NO formed and reduced via different pathways

Figure 10 shows the peak temperature and EINO during pure hydrogen MILD combustion diluted by 0-60%vol H_2O at 1 and 12 atm. As displayed in Figure 10, the peak temperature is reduced by less

than 100 K in the presence of 60%vol H_2O for both pressures, while a strong reduction of NO is observed with increasing H_2O dilution. The lower peak temperature in the presence of H_2O is largely caused by its physical effect at 1 and 12 atm, and such a physical effect is enhanced under high H_2O dilution conditions. However, regarding NO emission, the chemical effect of H_2O plays a stronger role in reducing the total EINO than the physical one over a wide range of X_{H_2O} from 0 to 60%.

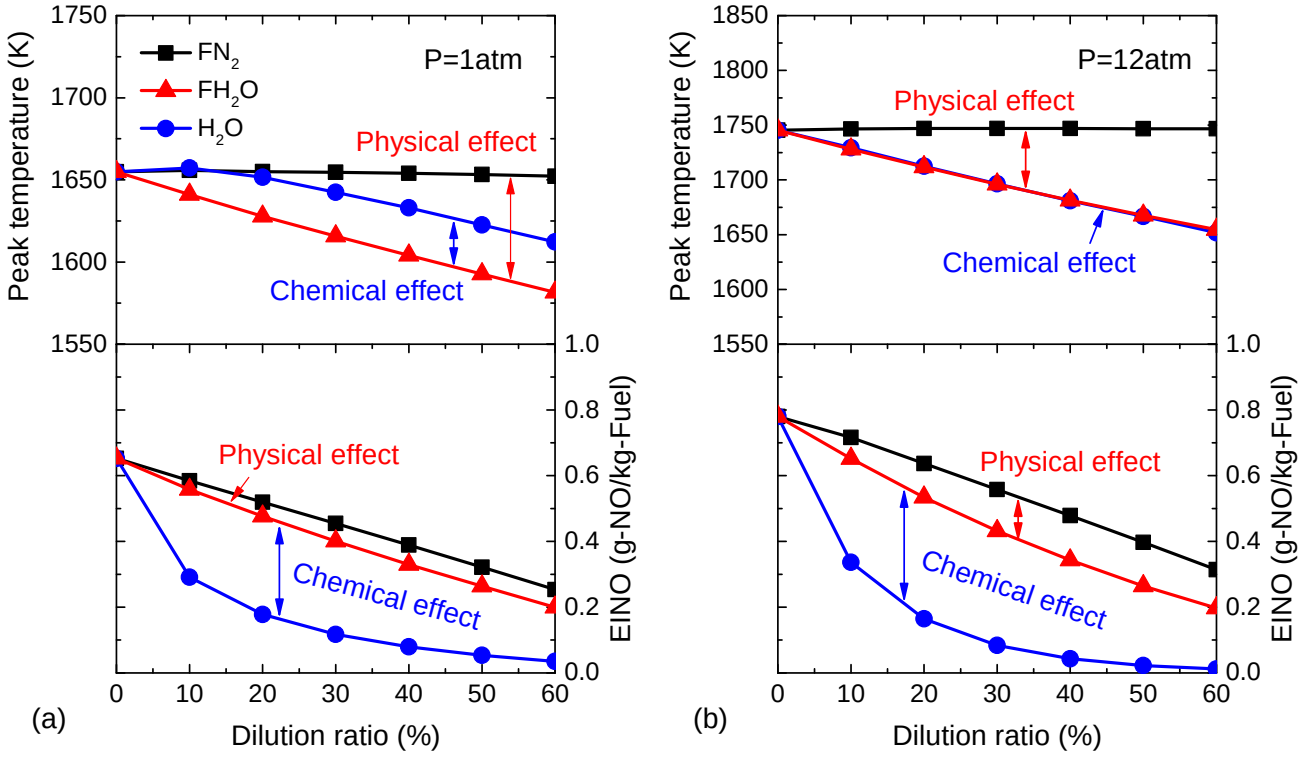

Figure 10. Peak temperature and NO mole fraction in pure hydrogen MILD combustion with H_2O dilution: (a) 1 atm, (b) 12 atm.

The physical and chemical effects of H_2O on the NO formed and reduced via different pathways are further analyzed in Figure 11. All the routes for either NO formation or NO destruction are significantly blocked with H_2O addition at both pressures. H_2O dilution constrains NO production by reducing the formation of O, H, and OH radicals (the main agents of NO production, which is also attested in Figure 5) mainly through its chemical effect, see Figure 12(a). The chemical effect of H_2O

437 on the O radicals proceeds through the reactions $H+O_2(+M)\rightleftharpoons HO_2(+M)$ (R13) and $OH+OH\rightleftharpoons O+H_2O$
438 (R5), as well as on the H radicals proceeds through the reactions $OH+H_2\rightleftharpoons H+H_2O$ (R4) and $O+H_2\rightleftharpoons$
439 OH+H (R3), further suppressing the rate of production and consumption of NO that comes from the
440 key steps NNH+O (R679), N_2O+H (R667), N_2O+O (R762), and NO+H (R720), as shown in Figure
441 12(b). And the effectiveness of the H_2O chemical role fades with H_2O addition up to 60%vol. Since
442 thermal NO is heavily dependent on temperature [62], H_2O dilution reduces the temperature caused
443 by higher specific heat capacity for H_2O relative to N_2, leading to the physical effect of H_2O mainly
444 responsible for the thermal NO reduction at high H_2O dilution through weakening the initiation
445 reaction $N_2+O\rightarrow NO$ (R674), as reflected by Figure 12(b).

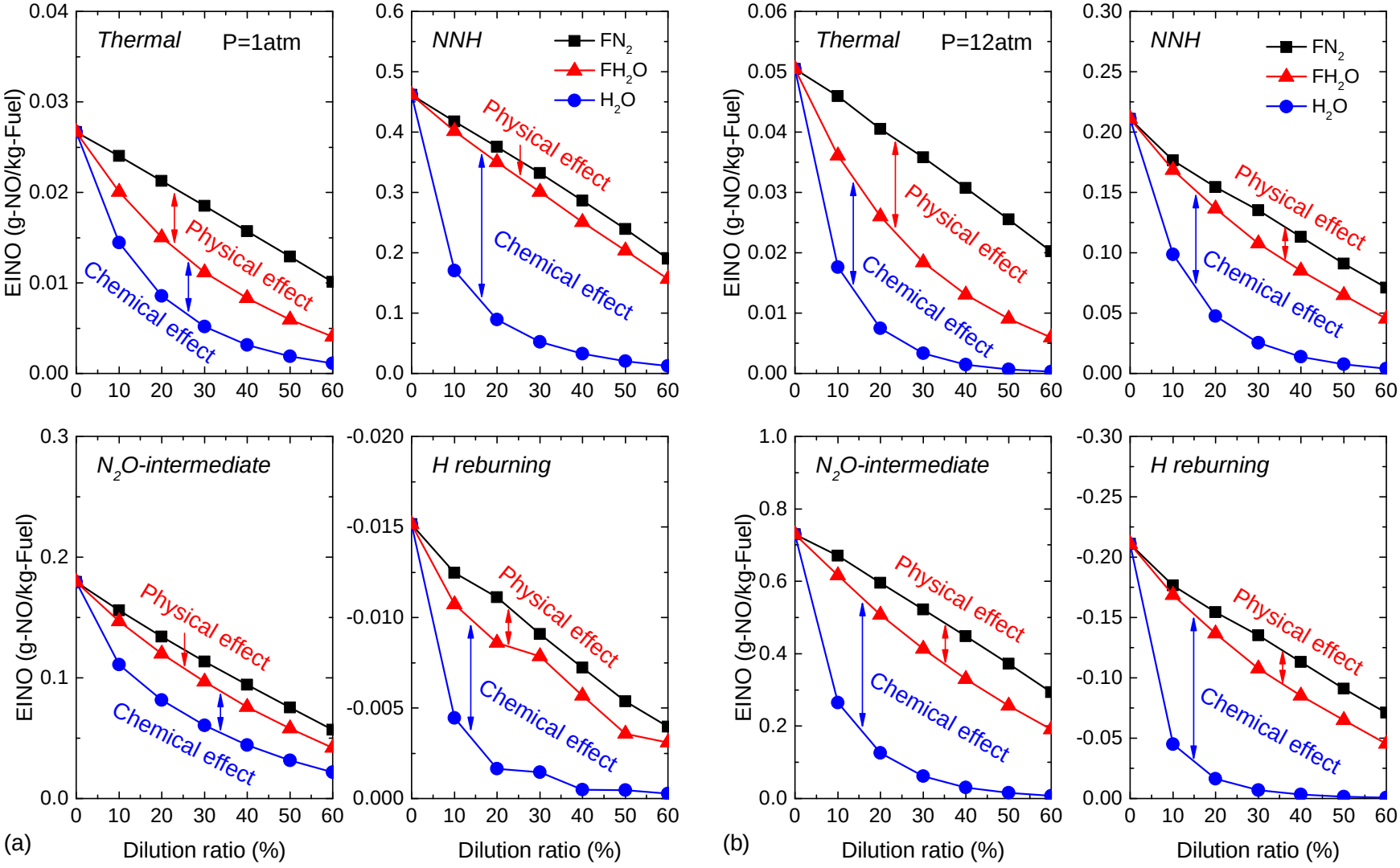

Figure 11. Physical and chemical effects of H_2O on the NO formed and reduced via different pathways in pure hydrogen MILD combustion: (a) 1 atm, (b) 12 atm.

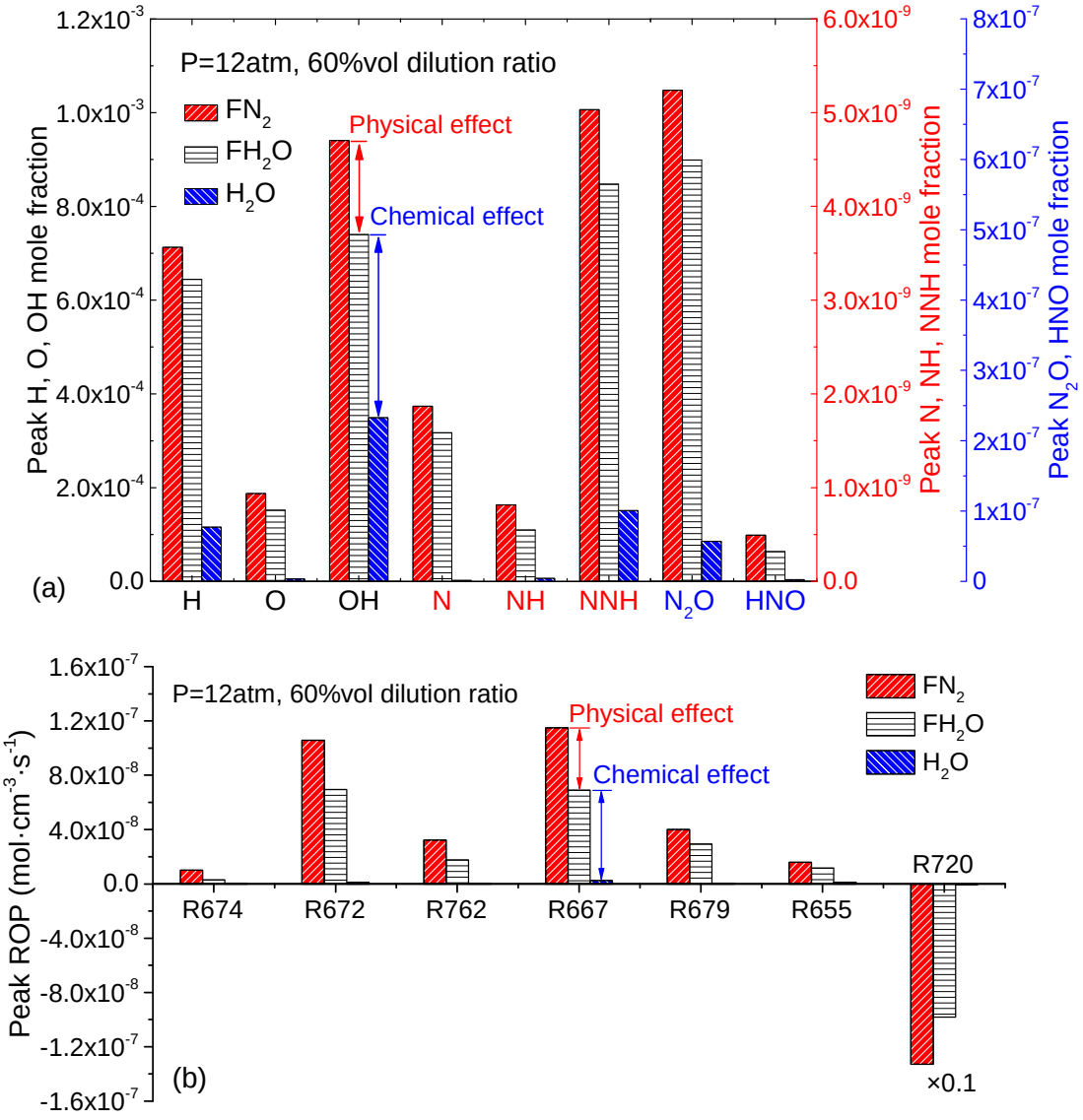

Figure 12. Physical and chemical effects of H_2O on the important NO-related (a) species and (b) reactions in pure hydrogen MILD combustion with 60%vol FN_2, FH_2O, or H_2O dilution at 12 atm.

In summary, H_2O dilution can further reduce NO emission in pure hydrogen MILD combustion at atmospheric and high pressures, primarily because of its chemical effect to play a role of holdback on the production of the H, O, OH, N, NH, N_2O, NNH, and HNO radical pools and then to slower the NO production rate. It is recommended to increase burner-inlet H_2O injection or strengthen in-furnace recirculation of burnt gases (mainly H_2O) to achieve further NO control/reduction for pure hydrogen

MILD combustion in industrial applications.

4.3.2. Relative importance of the thermal, NNH, N_2O-intermediate, and H reburning pathways

Figure 13 further presents the contribution of different sub-routes to the total NO production with H_2O dilution at 1 and 12 atm, where NO is formed primarily via the following two routes: NNH and N_2O. At 1 atm, H_2O dilution reduces the contribution of the NO formed via NNH while increasing that via N_2O, and the N_2O-intermediate route surpasses the NNH route to become the dominant NO formation route when H_2O dilution exceeds about 25%vol. The NO sensitivity analysis in Figure 14 shows that, as H_2O is added from 0 to 60%vol, the importance of the NO contributed by NNH+O→NO (R679) decreases and that contributed by $N_2O(+M)\rightleftharpoons N_2+O(+M)$ (R760) and $NH+NO\rightleftharpoons N_2O+H$ (R667) increases, which clarifies the evolution of the NNH and N_2O-intermediate pathways with H_2O dilution.

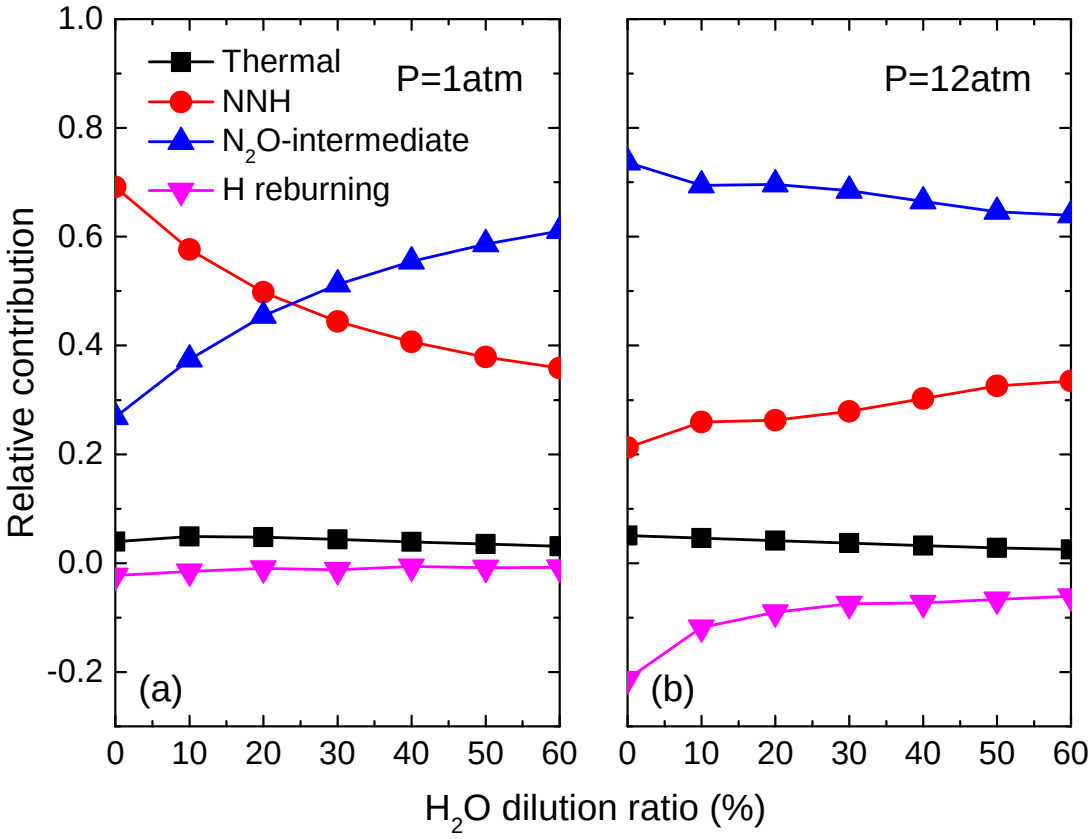

Figure 13. Variation of the contribution of different NO sub-pathways with H_2O dilution in pure hydrogen MILD combustion: (a) 1 atm, (b) 12 atm.

The response of the relative importance of different pathways to H_2O dilution at 12 atm follows a somewhat different trend at 1 atm, where the difference lies largely in that H_2O addition even up to 60%vol does not change the major NO formation pathway via N_2O at high pressure. At 12 atm, NO is formed mostly from the reaction of N_2O with H and O via $N_2O+H\rightarrow NH+NO$ (R667) and $N_2O+O\rightarrow NO+NO$ (R762), where N_2O is produced via the backward reaction of $N_2O(+M)\rightleftharpoons N_2+O(+M)$ (R760). The importance of these reactions in forming NO decreases if N_2 is replaced by H_2O. Therefore, the addition of H_2O weakens the effect of the N_2O-intermediate pathway, although it does not change the dominant role of the pathway via N_2O in NO formation. As for the NNH pathway, the channel $NNH+OH\rightarrow NO$ (R655) is more important than $NNH+O\rightarrow NO$ (R679) at high pressure. Despite lower

sensitivity for NNH+O→NO (R679) at high H_2O contents, H_2O dilution increases the sensitivity coefficient of NNH+OH→NO (R655), finally enhancing the importance of the NNH pathway with H_2O addition at high pressure. On the other hand, NO reduction by H atoms via NO+H(+M)⇌HNO(+M) (R720) is enhanced at high pressure, accounting for 21% at 12 atm without H_2O dilution (see Figure 13), while its contribution is weakened by 71.4% up to 6% when with the replacement of N_2 by H_2O at 60%vol. As H_2O is added, the H radical concentration is lowered largely due to its chemical effect and then the role of the initiation channel NO+H→HNO (R720) is suppressed in NO decomposition.

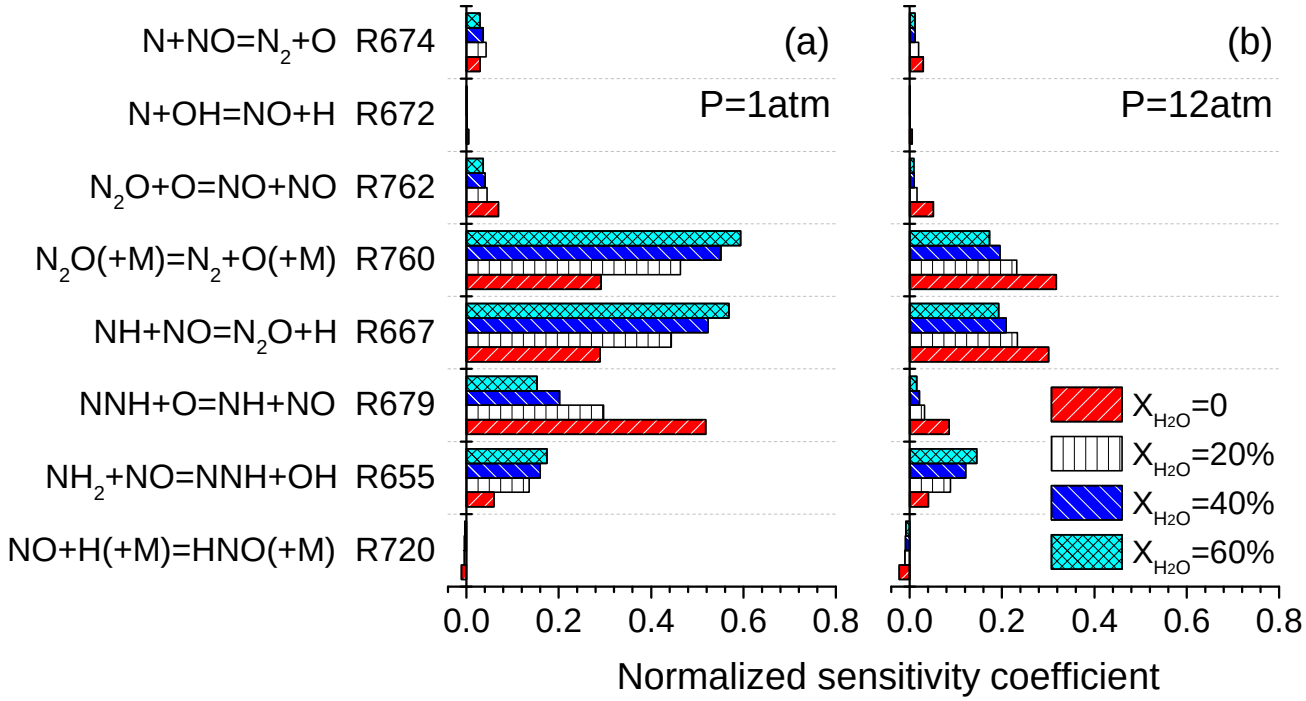

Figure 14. Sensitivity coefficient of the key NO reactions in pure hydrogen MILD combustion with H_2O dilution: (a) 1 atm, (b) 12 atm.

4.4. Evolution of the predominant NO forming or reducing pathway with pressure and H_2O dilution

Based on the above analysis, the major pathway of NO production or NO consumption is strongly dependent on pressure and H_2O dilution. Figure 15 further shows the evolution of the top contributor to NO formation as well as the importance of NO reduction by H radicals with pressure and H_2O dilution during pure hydrogen MILD combustion at X_{O_2}= 4%, T_o= 1200 K, φ= 1.0, and a_s= 100 s^{-1}. In Figure 15(a), the NNH route is found to be the dominant NO formation one under a low percentage of H_2O dilution at low pressures (e.g., < 3 atm), while the N_2O-intermediate pathway is the top NO contributor at high H_2O dilution levels or/and high pressures. Figure 15(b) reveals that NO reburning with H radicals is effective to reduce NO, and its role becomes more significant at high pressures, constituting about 21% of the total NO at 25 atm, whereas weakened by 71.4% from 21 to 6% with H_2O addition from 0 to 60%vol at 12 atm. It is suggested that how to cut off the N_2O-intermediate pathway as the top NO contributor needs to be addressed if further NO emission reduction is required under high-pressure or/and H_2O-diluted conditions.

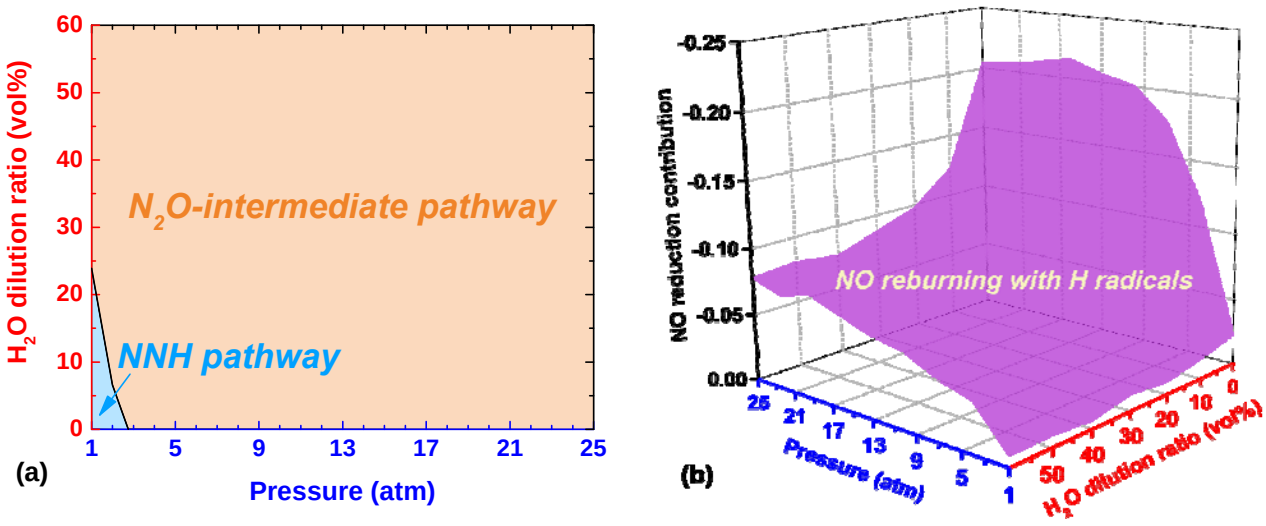

Figure 15. Evolution of the top contributor to (a) NO formation and (b) NO reduction with

pressure and H_2O dilution in pure hydrogen MILD combustion.

5. Conclusions

An opposed-flow diffusion flame model with Glarborg2018 is used to investigate NO reaction pathways in pure hydrogen MILD combustion. In particular, the present NO sub-pathway analysis method with Glarborg2018 for predicting thermal NO, prompt NO, NO formed via NNH and N_2O-intermediate pathways as well as NO reduced via CH_i and H reburning pathways is evaluated, and then the influence of pressure (1-25 atm) and H_2O dilution (0-60%vol) on NO formation and reduction via thermal, NNH, N_2O-intermediate, and H reburning pathways is analyzed, where the physical and chemical effects of H_2O are also identified. Important findings of the present study are given below.

(1) The present NO sub-pathway analysis method with Glarborg2018 can respectively predict thermal NO, prompt NO, NO formed via N_2O and NNH, and NO reduced via CH_i and H reburning pathways reasonably well.

(2) The EINO increases its peak with the pressure up to about 6 atm due to more NO formed via N_2O, and then starts to descent as the pressure is further increased up to 25 atm, which is mainly attributed to less NO formation via NNH and more NO reduction by H radicals, ultimately causing the dominant NO formation route to change from NNH to N_2O at high pressure.

(3) H_2O addition can achieve further NO emission reduction, which is primarily caused by the chemical effect of H_2O inhibiting the NNH and N_2O-intermediate pathways via the channels NNH+O/OH and N_2O+H/O to form NO. The dominant NO production route is changed from NNH to N_2O when H_2O dilution is larger than about 25%vol at atmospheric pressure, while

at high pressure, the N_2O-intermediate pathway is invariably the largest contributor to NO formation by H_2O dilution even up to 60%vol.

(4) NO reduction, which is initiated by reacting with H radicals mainly via the pathway $NO \xrightarrow{+H} HNO \xrightarrow{+H} NH \xrightarrow{+NO} N_2$, becomes more significant at high pressure, constituting 21% of the total NO produced at 25 atm, whereas its importance is decreased with H_2O dilution due to the chemical effect of H_2O to hinder H production and then to weaken the initiation channel NO+H(+M)⇌HNO(+M).

Acknowledgments

We acknowledge the financial support from the National Natural Science Foundation of China [grant number 51876074].

References

[1] Lu Y, Shao M, Zheng C, Ji H, Gao X, Wang Qg. Air pollutant emissions from fossil fuel consumption in China: Current status and future predictions. Atmospheric Environment. 2020;231:117536.

[2] Li B, Shi B, Zhao X, Ma K, Xie D, Zhao D, et al. Oxy-fuel combustion of methane in a swirl tubular flame burner under various oxygen contents: Operation limits and combustion instability. Experimental Thermal and Fluid Science. 2018;90:115-24.

[3] Cai T, Zhao D. Enhancing and assessing ammonia-air combustion performance by blending with dimethyl ether. Renewable and Sustainable Energy Reviews. 2022;156:112003.

[4] Christopher K, Dimitrios R. A review on exergy comparison of hydrogen production methods from renewable energy sources. Energy & Environmental Science. 2012;5:6640-51.

[5] Bothien MR, Ciani A, Wood JP, Fruechtel G. Toward decarbonized power generation with gas turbines by using sequential combustion for burning hydrogen. Journal of Engineering for Gas

Turbines and Power. 2019;141:121013.

[6] Sánchez AL, Williams FA. Recent advances in understanding of flammability characteristics of hydrogen. Progress in Energy and Combustion Science. 2014;41:1-55.

[7] Ji C, Zhao D, Li X, Li S, Li J. Nonorthogonality analysis of a thermoacoustic system with a premixed V-shaped flame. Energy Conversion and Management. 2014;85:102-11.

[8] Li L, Zhao D. Prediction of stability behaviors of longitudinal and circumferential eigenmodes in a choked thermoacoustic combustor. Aerospace Science and Technology. 2015;46:12-21.

[9] Zhao D, Li X. Minimizing transient energy growth of nonlinear thermoacoustic oscillations. International Journal of Heat and Mass Transfer. 2015;81:188-97.

[10] Zhao D, Li S, Zhao H. Entropy-involved energy measure study of intrinsic thermoacoustic oscillations. Applied Energy. 2016;177:570-8.

[11] Zhao D, Ang L, Ji CZ. Numerical and experimental investigation of the acoustic damping effect of single-layer perforated liners with joint bias-grazing flow. Journal of Sound & Vibration. 2015;342:152-67.

[12] Liang S, He J, Ji L, Zhao D. Identifying the skeleton mechanism for oscillatory combustion with functional weight analysis. Combustion and Flame. 2022;244:112243.

[13] Cavaliere A, de Joannon M. Mild combustion. Progress in Energy and Combustion Science. 2004;30:329-66.

[14] Tsuji H, Gupta AK, Hasegawa T, Katsuki M, Kishimoto K, Morita M. High temperature air combustion: from energy conservation to pollution reduction: CRC press; 2002.

[15] Wünning J, Wünning J. Flameless oxidation to reduce thermal NO-formation. Progress in Energy and Combustion Science. 1997;23:81-94.

[16] Arghode VK, Gupta AK. Effect of flow field for colorless distributed combustion (CDC) for gas turbine combustion. Applied Energy. 2010;87:1631-40.

[17] Perpignan AA, Rao AG, Roekaerts DJ. Flameless combustion and its potential towards gas turbines. Progress in Energy and Combustion Science. 2018;69:28-62.

[18] Flamme M. Low NO_x combustion technologies for high temperature applications. Energy Conversion and Management. 2001;42:1919-35.

[19] Flamme M. New combustion systems for gas turbines (NGT). Applied Thermal Engineering. 2004;24:1551-9.

[20] Nemitallah MA, Rashwan SS, Mansir IB, Abdelhafez AA, Habib MA. Review of novel combustion techniques for clean power production in gas turbines. Energy & Fuels. 2018;32:979-1004.

[21] Xing F, Kumar A, Huang Y, Chan S, Ruan C, Gu S, et al. Flameless combustion with liquid fuel: A review focusing on fundamentals and gas turbine application. Applied Energy. 2017;193:28-51.

[22] Khidr KI, Eldrainy YA, EL-Kassaby MM. Towards lower gas turbine emissions: Flameless distributed combustion. Renewable and Sustainable Energy Reviews. 2017;67:1237-66.

[23] Kruse S, Kerschgens B, Berger L, Varea E, Pitsch H. Experimental and numerical study of MILD combustion for gas turbine applications. Applied Energy. 2015;148:456-65.

[24] Levy Y, Sherbaum V, Arfi P. Basic thermodynamics of FLOXCOM, the low-NO_x gas turbines adiabatic combustor. Applied Thermal Engineering. 2004;24:1593-605.

[25] Lückerath R, Meier W, Aigner M. FLOX® combustion at high pressure with different fuel compositions. Journal of Engineering for Gas Turbines and Power. 2008;130.

[26] Schütz H, Lückerath R, Kretschmer T, Noll B, Aigner M. Analysis of the Pollutant Formation in the FLOX® Combustion. Journal of Engineering for Gas Turbines and Power. 2008;130.

[27] Huang M, Zhang Z, Shao W, Xiong Y, Lei F, Xiao Y. MILD combustion for hydrogen and syngas at elevated pressures. Journal of Thermal Science. 2014;23:96-102.

[28] Khalil AE, Gupta AK. Impact of pressure on high intensity colorless distributed combustion. Fuel. 2015;143:334-42.

[29] Lammel O, Schütz H, Schmitz G, Lückerath R, Stöhr M, Noll B, et al. FLOX® combustion at high power density and high flame temperatures. Journal of Engineering for Gas Turbines and Power. 2010;132.

[30] Zornek T, Monz T, Aigner M. Performance analysis of the micro gas turbine Turbec T100 with a new FLOX-combustion system for low calorific fuels. Applied Energy. 2015;159:276-84.

[31] Khalil HM, Eldrainy YA, Abdelghaffar WA, Abdel-Rahman AA. Increased heat transfer to sustain

flameless combustion under elevated pressure conditions–a numerical study. Engineering Applications of Computational Fluid Mechanics. 2019;13:782-803.

[32] Sadanandan R, Lückerath R, Meier W, Wahl C. Flame characteristics and emissions in flameless combustion under gas turbine relevant conditions. Journal of Propulsion and Power. 2011;27:970-80.

[33] Shi G, Li P, Hu F, Liu Z. NO mechanisms of syngas MILD combustion diluted with N_2, CO_2, and H_2O. International Journal of Hydrogen Energy. 2022.

[34] Park J, Choi JW, Kim SG, Kim KT, Keel SI, Noh DS. Numerical study on steam‐added mild combustion. International Journal of Energy Research. 2004;28:1197-212.

[35] Jonsson M, Yan J. Humidified gas turbines—a review of proposed and implemented cycles. Energy. 2005;30:1013-78.

[36] de Joannon M, Sabia P, Cozzolino G, Sorrentino G, Cavaliere A. Pyrolitic and oxidative structures in hot oxidant diluted oxidant (HODO) MILD combustion. Combustion Science and Technology. 2012;184:1207-18.

[37] Cheong K-P, Li P, Wang F, Mi J. Emissions of NO and CO from counterflow combustion of CH_4 under MILD and oxyfuel conditions. Energy. 2017;124:652-64.

[38] Shu Z, Dai C, Li P, Mi J. Nitric oxide of MILD combustion of a methane jet flame in hot oxidizer coflow: Its formations and emissions under H_2O, CO_2 and N_2 dilutions. Fuel. 2018;234:567-80.

[39] Si J, Wang G, Shu Z, Liu X, Wu M, Zhu R, et al. Experimental and Numerical Study on Moderate or Intense Low-Oxygen Dilution Oxy-Combustion of Methane in a Laboratory-Scale Furnace under N_2, CO_2, and H_2O Dilutions. Energy & Fuels. 2021.

[40] Xu S, Tong Y, Jin S, Ren H, Tu Y, Zhang S, et al. NO formation and reduction during methane/hydrogen MILD combustion over a wide range of hydrogen-blending ratios in a well-stirred reactor. Fuel. 2023;346:128324.

[41] Moliere M, Hugonnet N, Energy G. Hydrogen-fuelled gas turbines: Experience and Prospects. Power-Gen Asia. 2004.

[42] Yuri M, Masada J, Tsukagoshi K, Ito E, Hada S. Development of 1600 C-class high-efficiency gas turbine for power generation applying J-Type technology. Mitsubishi Heavy Industries

Technical Review. 2013;50:1-10.

[43] Glarborg P, Kristensen PG, Dam-Johansen K, Alzueta M, Millera A, Bilbao R. Nitric oxide reduction by non-hydrocarbon fuels. Implications for reburning with gasification gases. Energy & Fuels. 2000;14:828-38.

[44] Glarborg P, Miller JA, Ruscic B, Klippenstein SJ. Modeling nitrogen chemistry in combustion. Progress in Energy and Combustion Science. 2018;67:31-68.

[45] Design R. Chemkin-pro 15101. Reaction Design, San Diego, CA. 2010.

[46] Puri I, Seshadri K. Extinction of diffusion flames burning diluted methane and diluted propane in diluted air. Combustion and Flame. 1986;65:137-50.

[47] Bowman CT, Hanson RK, Davidson DF, Gardiner Jr. WC, Lissianski V, Smith GP. GRI-Mech 2.11. http://combustion.berkeley.edu/gri-mech/new21/version21/text21.html.

[48] Smith GP, Golden DM, Frenklach M, Moriarty NW, Eiteneer B, Goldenberg M. GRI-Mech 3.0. http://combustion.berkeley.edu/gri-mech/version30/text30.html.

[49] Li J, Zhao Z, Kazakov A, Dryer FL. An updated comprehensive kinetic model of hydrogen combustion. International journal of chemical kinetics. 2004;36:566-75.

[50] Davis SG, Joshi AV, Wang H, Egolfopoulos F. An optimized kinetic model of H_2/CO combustion. Proceedings of the Combustion Institute. 2005;30:1283-92.

[51] Wang H, You X, Joshi AV, Davis SG, Laskin A, Egolfopoulos F, et al. USC Mech Version II. High-temperature combustion reaction model of H_2/CO/C_1-C_4 compounds. URL: http: //ignis usc edu/USC_Mech_II htm. 2007.

[52] Konnov A. Implementation of the NCN pathway of prompt-NO formation in the detailed reaction mechanism. Combustion and Flame. 2009;156:2093-105.

[53] Rørtveit GJ, Hustad JE, Li S-C, Williams FA. Effects of diluents on NO_x formation in hydrogen counterflow flames. Combustion and Flame. 2002;130:48-61.

[54] de Persis S, Idir M, Molet J, Pillier L. Effect of hydrogen addition on NO_x formation in high-pressure counter-flow premixed CH_4/air flames. International Journal of Hydrogen Energy. 2019;44:23484-502.

[55] Xu S, Jin S, Tong Y, Shi B, Tu Y, Liu H. Quantitative evaluation of NO formation and destruction

routes during methane MILD combustion using an improved calculation method. Fuel. 2022;324:124593.

[56] Engleman V, Bartok W, Longwell J, Edelman R. Experimental and theoretical studies of NO_x formation in a jet-stirred combustor. Symposium (International) on Combustion: Elsevier; 1973. p. 755-65.

[57] Bartok W, DEL VALLE E. Basic kinetic studies and modeling of nitrogen oxide formation in combustion processes. 1972.

[58] Xie L, Hayashi S, Hirose K. NO_x formation in turbulent lean-premixed combustion with minimum heat losses. Symposium (International) on Combustion: Elsevier; 1996. p. 2155-60.

[59] Purohit AL, Nalbandyan A, Malte PC, Novosselov IV. NNH mechanism in low-NO_x hydrogen combustion: Experimental and numerical analysis of formation pathways. Fuel. 2021;292:120186.

[60] Chen AT, Malte PC. Influence of fuel-N compound type and SO_2 on nitrogen reactions in stirred flames. paper WSS/CT 84-86, Western States Section Meeting of the Combustion Instite1984.

[61] Dayma G, Dagaut P. Effects of air contamination on the combustion of hydrogen—effect of NO and NO_2 addition on hydrogen ignition and oxidation kinetics. Combustion Science and Technology. 2006;178:1999-2024.

[62] Zeldovich YB. The oxidation of nitrogen in combustion and explosions. Acta Physicochim URSS. 1946;21:577-628.

[63] Konnov A. On the relative importance of different routes forming NO in hydrogen flames. Combustion and Flame. 2003;134:421-4.

[64] Bowman CT. Control of combustion-generated nitrogen oxide emissions: technology driven by regulation. Symposium (International) on Combustion: Elsevier; 1992. p. 859-78.

[65] Bozzelli JW, Dean AM. O+NNH: A possible new route for NO_x formation in flames. International Journal of Chemical Kinetics. 1995;27:1097-109.

[66] Fenimore CP. Formation of nitric oxide in premixed hydrocarbon flames. Symposium (International) on Combustion: Elsevier; 1971. p. 373-80.

[67] Wendt JO, Sternling C, Matovich M. Reduction of sulfur trioxide and nitrogen oxides by secondary fuel injection. Symposium (International) on Combustion: Elsevier; 1973. p. 897-

904.

[68] Pons L, Darabiha N, Candel S. Pressure effects on nonpremixed strained flames. Combustion and Flame. 2008;152:218-29.

[69] Ni S, Zhao D. NO_x emission reduction in ammonia-powered micro-combustors by partially inserting porous medium under fuel-rich condition. Chemical Engineering Journal. 2022;434:134680.

[70] Cai T, Zhao D. Temperature dependence of laminar burning velocity in ammonia/dimethyl ether-air premixed flames. Journal of Thermal Science. 2022;31:189-97.

[71] Takeno T, Nishioka M. Species conservation and emission indices for flames described by similarity solutions. Combustion and Flame. 1993;92:465-8.

[72] Klippenstein SJ, Harding LB, Glarborg P, Miller JA. The role of NNH in NO formation and control. Combustion and Flame. 2011;158:774-89.